MOMENTUM, MASS, HEAT, AND VORTICITY BALANCES FROM OCEANIC MEASUREMENTS OF CURRENT AND TEMPERATURE

by

HARRY LEONARD BRYDEN JR.

A.B., Dartmouth College
(1968)

SUBMITTED IN PARTIAL FULFILLMENT OF THE
REQUIREMENTS FOR THE DEGREE OF
DOCTOR OF PHILOSOPHY

at the

MASSACHUSETTS INSTITUTE OF TECHNOLOGY

and the

WOODS HOLE OCEANOGRAPHIC INSTITUTION

July, 1975

Signature of Author.....
Joint Program in Oceanography, Massachusetts Institute of Technology-Woods Hole Oceanographic Institution, and Department of Earth and Planetary Sciences, and Department of Meteorology, Massachusetts Institute of Technology, July, 1975

Certified by.....
Thesis Supervisor

Accepted by.....
Chairman, Joint Oceanography Committee in the Earth Sciences, Massachusetts Institute of Technology-Woods Hole Oceanographic Institution

MOMENTUM, MASS, HEAT, AND VORTICITY BALANCES FROM OCEANIC MEASUREMENTS OF CURRENT AND TEMPERATURE

by

Harry Leonard Bryden Jr.

Submitted to the Massachusetts Institute of Technology-Woods Hole Oceanographic Institution Joint Program in Oceanography on July 25, 1975, in partial fulfillment of the requirements for the degree of Doctor of Philosophy

ABSTRACT

The local dynamics of low-frequency motions in the MODE region are investigated from three arrays of moored measurements of current and temperature. Tests for lowest-order balances of horizontal momentum, mass, heat, and vorticity within estimated errors are carried out.

Geostrophic comparisons of four-day averaged observed and geostrophic current differences from the MODE-1 array indicate that a geostrophic balance within estimated errors is the lowest-order horizontal momentum balance. The discrepancy between observed and geostrophic current differences has a standard deviation of 1.9 cm/sec which is 26% as large as the standard deviation of the current differences. In the mass balance, comparisons of estimates of $\frac{\partial u}{\partial x}$ and $\frac{\partial v}{\partial y}$ from the MODE-0 Array 1 indicate that within estimated errors the low-frequency currents are horizontally nondivergent. The standard deviation of horizontal divergence, which is the discrepancy from horizontal nondivergence, is $.22 \times 10^{-6}$ sec^{-1} which is 36% as large as the standard deviation of the estimates of horizontal derivatives of velocity. These tests significantly increase the observational basis for geostrophy and horizontal nondivergence and confirm the validity of the error estimates.

In the heat balance, estimates of horizontal advection of temperature balance local time changes of temperature within estimated errors for the IWEX observations. These estimates have small errors because a representation of horizontal advection of temperature in terms of the speed and turning about the vertical of the horizontal current is used. The errors are so small that from future measurements it may be possible to estimate the sum of local change plus horizontal advection of temperature and from this sum it may be possible to estimate vertical velocity.

This balance between local change and horizontal advection demonstrates that horizontal advection of spatially-varying features is an important cause of local time changes. The horizontal advection could not be explained in terms of advection by the long time-averaged flow field. This suggests that the local dynamics of low-frequency motions in

the MODE region are strongly nonlinear. An indication of energy transfer, which occurs in nonlinear processes, is found in a phase lag such that estimates of horizontal advection lead local changes of temperature. In the context of the baroclinic instability model this phase lag is consistent with the growth of perturbation wave energy by conversion of potential energy contained in the forty-day averaged flow field.

In the vorticity balance, estimates of planetary advection account for only half the local time change of vorticity for MODE-0 Array 1 measurements. Within estimated errors these two terms do not balance, so these observations cannot be explained as manifestations of barotropic Rossby waves alone. Estimates of vortex stretching and horizontal advection of relative vorticity could not be made. A phase lag such that estimates of planetary advection lead local changes of vorticity is consistent in the context of the instability model with an increase in perturbation wave enstrophy, which must occur when the perturbation wave grows, due to the conversion of planetary enstrophy.

Because of the importance of the vorticity balance for understanding the dynamics of low-frequency motions an experiment is suggested to estimate accurately all terms in the lowest-order vorticity balance. From such measurements the energy transfer and enstrophy conversion could also be estimated.

Thesis Supervisor: Nick P. Fofonoff
Title: Senior Scientist in
Physical Oceanography

ACKNOWLEDGEMENTS

Throughout this thesis work Dr. Nick Fofonoff has provided guidance and encouragement. His subtle suggestions often were not understood until months later. His equanimity was much appreciated during the periodic intervals of doubt and despair.

Dr. William Schmitz kicked me hard and often and, though it still hurts, I am sure the advice will serve me well in the future. He quickly identified the important sections of the work and demanded that I extend the interpretation as far as possible. Prof. John Hart's criticism was most helpful in isolating the sections which required clarification.

Other members of my thesis committee who provided stimulation and criticism include Drs. Norman Phillips, John Gould, Henry Stommel, and Ferris Webster. Drs. Bruce Warren, Carl Wunsch, and Nelson Hogg read the thesis carefully and their suggestions helped improve many sections.

I gratefully acknowledge the financial support which allowed me to complete my graduate work. Support to carry out this thesis work was provided by the Office of Naval Research under contracts N00014-66-C0241 and C0262 NR 083-004 and by the National Science Foundation Office of the International Decade of Ocean Exploration under grant ID075-03962. During my graduate career, support was also provided by the National Science Foundation under grants GA 21172 and DES74-19782 and by the Woman's Seamen's Friend Society of Connecticut under a Summer Fellowship.

Drs. W. Schmitz and C. Wunsch and Drs. M. Briscoe and K. Hasselmann kindly allowed me to use their MODE and IWEX measurements respectively at a very early stage of the processing. The quality of these current and temperature measurements is a tribute to the members of the WHOI Buoy Group who work so successfully at sea. Dr. W. Schmitz has provided an important stimulus for the improvement of the subsurface mooring measurements. The MODE measurements were made through the support of the Office of Naval Research under contracts N00014-66-C0241 and C0262 NR 083-004 and of the National Science Foundation Office of the International Decade of Ocean Exploration under grants GX-29054 and GX-29034. The IWEX measurements were made through the support of The Johns Hopkins University Applied Physics Laboratory under subcontract 372111.

J. Dean, R. Payne, and especially S. Tarbell were helpful in assessing the quality of measurements. J. Maltais and D. Chausse explained the computer's idiosyncracies in very simple terms. With great perseverance R. Millard and D. Moore showed me how to use a wrench at sea. R. Thompson taught me the ways of the world and H. Stommel taught me that even traffic patterns on the Southeast Expressway can be used to understand water motions.

Philosophical conversations with Brad Butman and Kuh Kim were stabilizing influences.

The meticulous typing of Audrey Williams is self-evident. She patiently typed draft after draft.

Without the enthusiasm of Cindy and the joy of Cyrus this work could not have been completed.

TABLE OF CONTENTS

		Page
ABSTRACT		2
ACKNOWLEDGMENTS		4
LIST OF FIGURES		7
LIST OF TABLES		8
CHAPTER I	INTRODUCTION	9
CHAPTER II	HORIZONTAL MOMENTUM BALANCE: GEOSTROPHY	
	Introduction	23
	Theory	24
	Data and Methods	30
	Results and Discussion	36
	Conclusions	50
CHAPTER III	MASS BALANCE: HORIZONTAL NONDIVERGENCE	
	Introduction	52
	Theory	53
	Data and Methods	54
	Results and Discussion	59
	Conclusions	72
CHAPTER IV	HEAT BALANCE: HORIZONTAL ADVECTION OF TEMPERATURE	
	Introduction	73
	Theory	75
	Data and Methods	78
	Results and Discussion	80
	Conclusions	97
CHAPTER V	VORTICITY BALANCE	
	Introduction	98
	Theory	99
	Data and Methods	100
	Results and Discussion	109
	Conclusions	115
CHAPTER VI	CONCLUSIONS	117
REFERENCES		122
BIOGRAPHY AND PUBLICATIONS		130

LIST OF FIGURES

Figure		Page
1.1	Spatial distribution of MODE-1 moorings. . .	14
1.2	Spatial distribution of MODE-0 Array 1 moorings	16
2.1	Daily observed current difference plotted against estimates of geostrophic current difference for all MODE-1 geostrophic comparisons.	39
2.2	Comparison of observed and geostrophic current differences for MODE-1 moorings 3 and 6	46
3.1	Daily estimates of $\frac{\partial v}{\partial y}$ plotted against estimates of $\frac{\partial u}{\partial x}$ from MODE-0 Array 1 measurements	60
3.2	Horizontal derivatives of velocity as a function of time during MODE-0	64
4.1	Four-day averaged estimates of local time change of temperature and negative horizontal advection of temperature from IWEX measurements.	81
4.2	Daily estimates of local time change and negative horizontal advection of temperature	84
4.3	Four-day averaged estimates of local time change and negative horizontal advection of temperature with error estimates.	88
5.1	Daily estimates of relative vorticity, $\frac{\partial v}{\partial x} - \frac{\partial u}{\partial y}$, from MODE-0 Array 1 measurements of velocity at 1500 m depth.	101
5.2	Map of relative vorticity from MODE-1 measurements of velocity at 420 m depth during the period 21-28 April, 1973.	107

LIST OF TABLES

Table		Page
2.1	Results of thermal wind correlations from MODE-1 measurements	37
2.2	Geostrophic comparisons from MODE-1 measurements.	42
3.1	MODE-0 Array 1 data used in tests for horizontal nondivergence.	55
3.2	Tests for horizontal nondivergence from four-day averaged estimates of $\frac{\partial u}{\partial x}$ and $\frac{\partial v}{\partial y}$ from MODE-0 Array 1 measurements.	62
3.3	Comparison of direct and indirect estimates of horizontal divergence from MODE-0 Array 1 measurements.	67
3.4	Divergence ratio calculated for various time averaging intervals from MODE-0 Array 1 measurements.	70
4.1	Comparison of local time change and horizontal advection of temperature over four-day periods during IWEX.	86
5.1	Comparison of local time change of vorticity with advection of planetary vorticity for MODE-0 Array 1 measurements	103
5.2	Comparison of the sum of local time change of vorticity plus advection of planetary vorticity with vortex stretching for MODE-0 Array 1 measurements.	105

CHAPTER I

INTRODUCTION

This thesis presents an analysis of dynamic and kinematic balances for low-frequency oceanic motions from measurements of current and temperature. Low-frequency motions are those with periods longer than the local inertial period. The balances examined are the horizontal momentum, mass, heat and vorticity balances. Not all terms in each balance are estimated. The equations are scaled and the largest terms are estimated and tested for balance.

This thesis is written such that each of Chapters II, III, IV, and V is a self-contained analysis of a particular balance. Tests for geostrophy as the lowest order balance in the horizontal momentum equations are described in Chapter II. In Chapter III the tests for horizontal non-divergence as the lowest-order mass balance are described. Tests for balance between local changes of temperature and horizontal advection of temperature in the heat equation are the subject of Chapter IV. A discussion of the feasibility of estimating vorticity balances from measurements and a test for balance between local change of vorticity and advection of planetary vorticity are contained in Chapter V. Chapter VI summarizes the results of all balance tests and their importance. This introductory chapter provides the motivation and background for the balance tests.

Each of Chapters II, III, IV and V includes five sections: introduction, theory, data and methods, results and discussion, and conclusions. In each introduction the importance of the balance calculations is outlined. In the theory section the conservation equation is scaled and the lowest-order balance isolated. In the section of data and methods the calculations and their errors are outlined. The section of results and discussion includes a statement of the results, comparisons with related work, and a discussion of the feasibility of a higher-order balance test. The conclusions section summarizes the major results of each balance test.

The measurements used in this analysis were made southwest of Bermuda in the western North Atlantic. The low-frequency currents in this region are dominated by motions of time scale of order 20 days and horizontal length scales of order 100 km (Gould, Schmitz and Wunsch, 1974) which are called eddies during the Mid-Ocean Dynamics Experiment (MODE). These eddies, first observed by Swallow (1971), contain much greater kinetic energy than mid-ocean mean currents. It is the local dynamics of these low-frequency currents in the form of their lowest-order horizontal momentum, mass, heat and vorticity balances which is studied in this work. Knowledge of the local dynamics of eddies is certainly important for predicting distributions of momentum, heat and vorticity over periods at least as long as one month. In addition, it is an axiom of MODE that only by

understanding the local dynamics of eddies can their effect on mean currents be parameterized properly in models of mean ocean circulation (MODE Scientific Council, 1973).

There are several motivations for this work. The first is to provide an observational basis for the lowest-order balances of geostrophy in the horizontal momentum equations and horizontal nondivergence in the mass balance. Although these balances are expected on theoretical grounds, there are few direct tests of these balances. Only a few geostrophic comparisons by Swallow (1971) using modern current measurements are available. And only one rather unsuccessful attempt by Shonting (1969) to examine the mass balance from direct current measurements is available. The tests for geostrophy (Chapter II) and horizontal nondivergence (Chapter III) presented here then significantly increase the observational basis for these balances.

A second motivation is to provide guidance to theoretical and numerical modelers. The relative importance of terms in the analyses of heat (Chapter IV) and vorticity (Chapter V) balances, where the lowest-order balances are not theoretically determined, should be valuable information for decisions on the inclusion or neglect of terms in future models. Because the balances examined here are the basis for all models, these results also provide a means of evaluating the applicability of existing models for explaining the observations.

The most important motivation for this work is to answer basic dynamical questions from the measurements to further the understanding of ocean physics. The foremost questions in the dynamics of low-frequency motions whose answers are sought here are:

1. How important is horizontal advection relative to local time changes?

2. How important are the β-effect and vortex stretching in the vorticity balance relative to local time changes of vorticity?

3. Does energy transfer occur?

The value of this work in understanding the dynamics of low-frequency currents is contained in the answers to these questions. That local time changes of temperature are balanced by horizontal advection of temperature (Chapter IV) demonstrates that horizontal advection causes local time changes of temperature and perhaps of momentum, vorticity and energy for low-frequency currents. That planetary advection balances only half the local time change of vorticity (Chapter V) demonstrates that, while it is important in causing local changes, the β-effect is not the only important cause of local change of vorticity. The indications of phase lags in time such that estimates of horizontal advection of temperature lead local changes of temperature (Chapter V) are consistent in the context of the baroclinic instability model with the growth of a perturbation wave by conversion of energy contained in the mean flow field. In ad-

dition, an extended error analysis suggests that a future experiment could be carried out to estimate accurately each term in the vorticity balance and to calculate the transfer of energy (Chapter V).

There is a philosophical problem in answering these questions from observations in that the answers are valid only for the particular data set. Usually it is assumed that extrapolations to general conclusions can be made after several studies yield similar results. It is assumed here that the results from a single data set are characteristic of the MODE region so that implications of the results can be explored. The observations may be anomalous so that the generalizations should be tested by later studies. In truth, the answers to these questions and the conclusions of this thesis are specific for the observations examined.

Three different arrays are used in this work because each has its particular advantage. The advantage of the MODE-1 array (Figure 1.1), which was designed to describe an eddy and to investigate eddy dynamics (MODE Scientific Council, 1973; Tarbell, 1975a), is the combination of current and temperature measurements at several depths on sixteen moorings which allows geostrophic comparisons to be made in Chapter II. The MODE-0 Array 1 (Figure 1.2), designed to estimate the temporal and spatial scales of low-frequency motions in the MODE region (Gould, Schmitz and Wunsch, 1974; Tarbell, 1975c), had current meters at 1500 m depth on four moorings separated horizontally by shorter distances than in

Figure 1.1. Spatial distribution of MODE-1 moorings

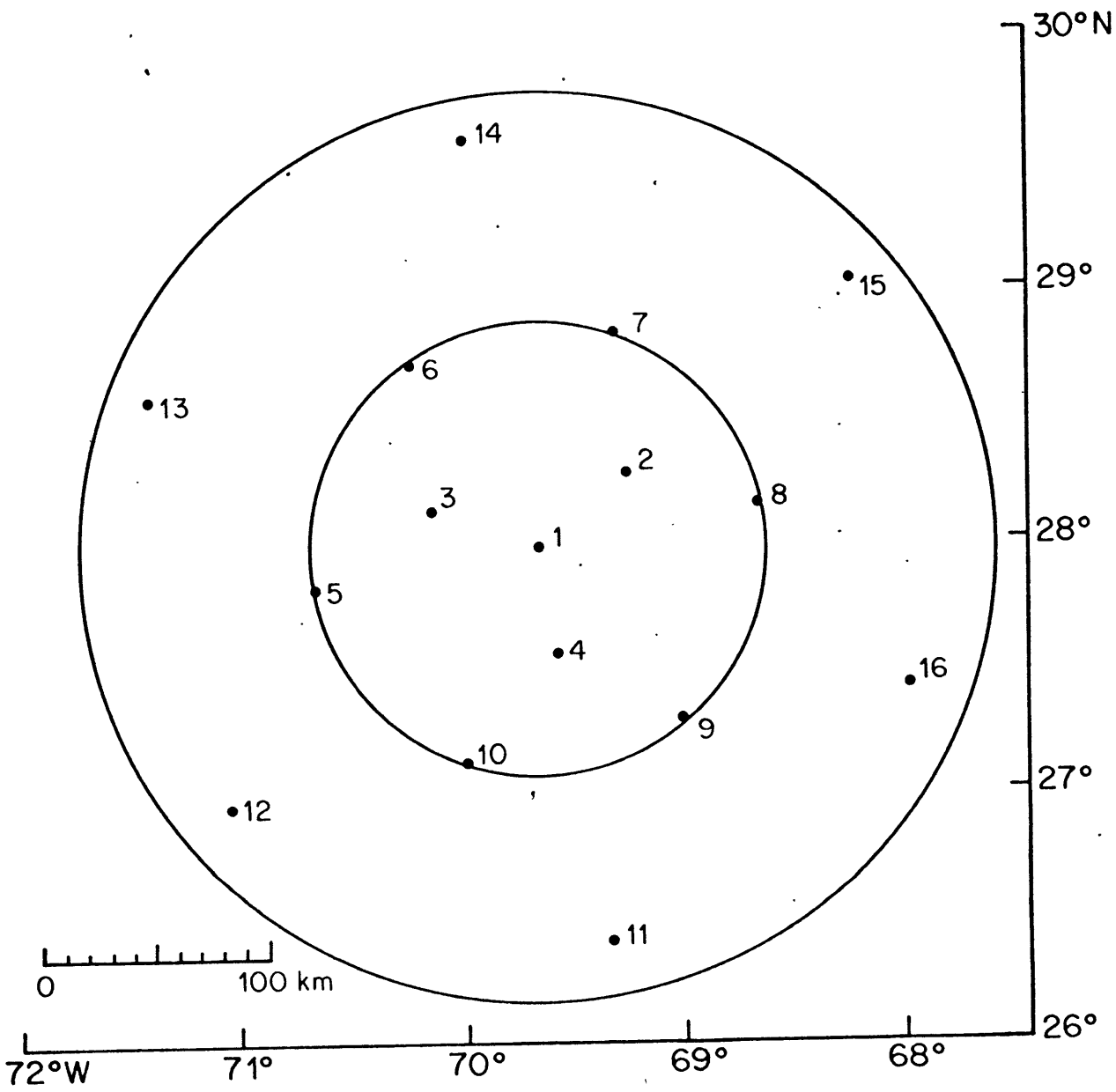
30°N
29°
28°
27°
26°
72°W
71°
70°
69°
68°
1
2
3
4
5
6
7
8
9
10
11
12
13
14
15
16
0
100 km

Figure 1.2. Spatial distribution of MODE-0 Array 1 moorings.

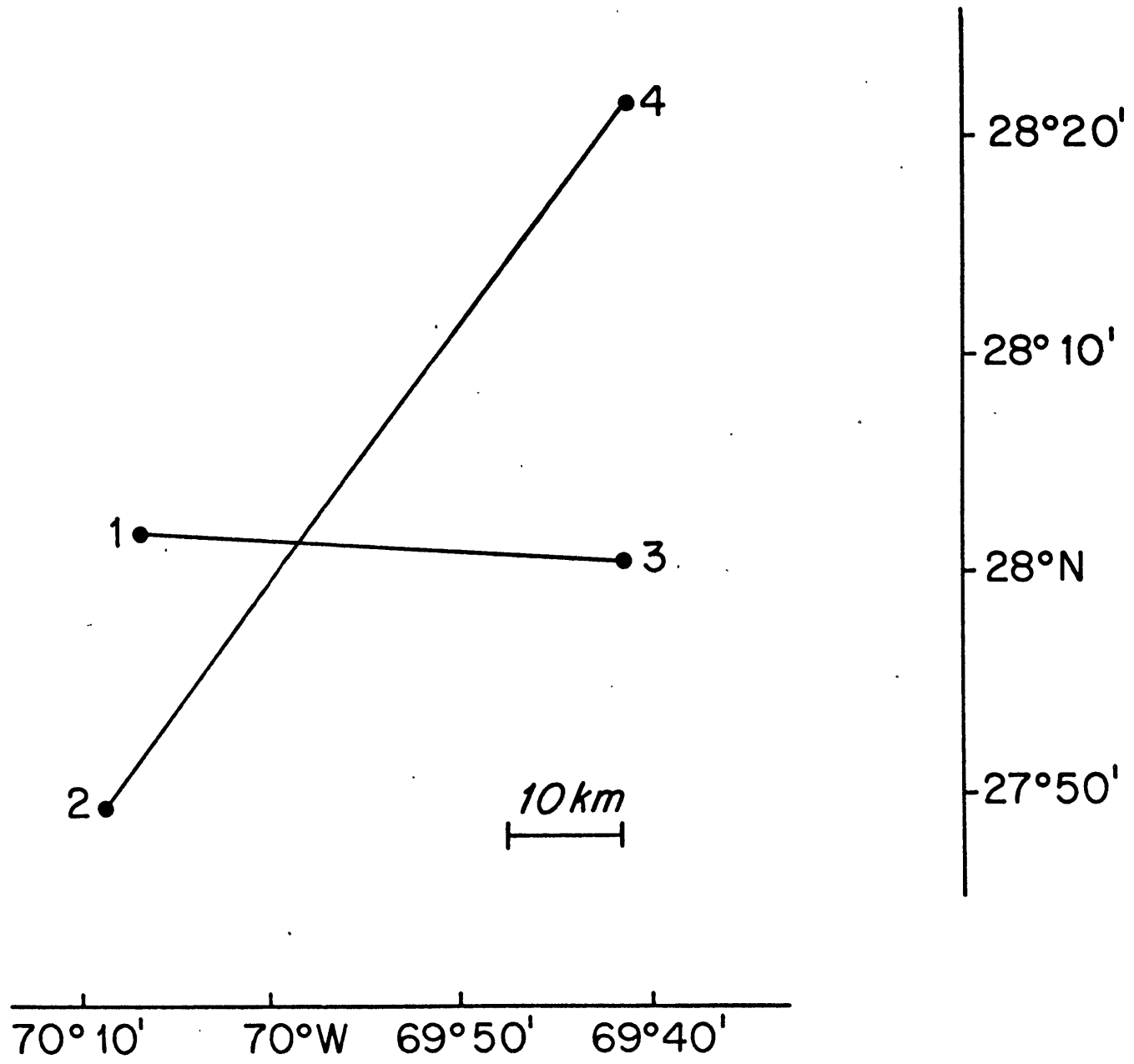
4
1
3
2
10km
28°20'
28° 10'
28°N
27°50'
70° 10'
70°W
69°50'
69°40'

the MODE-1 array. These shorter separations allow more accurate estimates of horizontal derivatives of velocity to be made so that tests for horizontal nondivergence (Chapter III) and for a vorticity balance (Chapter V) could be made within smaller errors. The IWEX array, designed to investigate the frequency-wavenumber spectrum of internal waves (Briscoe, 1975; Tarbell, 1975b), had three measurements of current and temperature at each of six depths on a mooring in the shape of a tetrahedron. These measurements allow accurate estimates of horizontal advection of temperature to be made and compared with local time changes of temperature (Chapter IV).

In order to use these measurements in balance tests for low-frequency motions, they are averaged in time by putting them through a Gaussian filter of half-width twenty-four hours, designed by Schmitz (1974) to eliminate internal-inertial motions, and subsampling daily values. This averaging procedure decreases by 98% the amplitude of inertial motions, which are the major contamination in the estimates of low-frequency currents, and yields independent data points approximately every twenty-eight hours (Briscoe, private communication). Calculations requiring many data points, such as correlations, are made from the daily values. For comparisons involving magnitudes of terms, an averaging of the daily values over four days is carried out to filter out more completely the higher-frequency fluctuations. Estimates of derivatives are made by finite differencing and estimates of integrals are made by the trapezoidal rule.

The results of this study depend critically on the size and accuracy of the estimated errors. If the estimated errors are large the conclusions are weak since any terms balance within large enough errors. The particular advantage discussed above for each of the three arrays is that the estimated errors for a particular balance test are smallest for that array. Accurate error estimates are needed to ensure that invalid conclusions are not made because the error estimates are too small. Oceanographers are fortunate to have several balances, including geostrophy and horizontal nondivergence, which are so well-defined on theoretical grounds that they can be tested within estimated errors as a means of confirming the accuracy of the estimated errors.

Errors are considered to be of three types: instrumental, sampling and theoretical. Instrumental errors are due to the varying response of the sensors. To obtain values of these errors it is assumed that four-day averages of current and temperature from current meters separated horizontally by small distances (6 m to 1600 m) on the IWEX mooring should be the same. Standard deviations of the differences are .032°C in temperature, .50 cm/sec in speed, and .074 radians in direction. Differences in changes of temperature over four days have standard deviation .004°C indicating that most of the temperature differences are due to bias errors. These standard deviations are divided by $\sqrt{2}$ and used as instrumental errors.

Sampling errors arise from having measurements at discrete points in a continuous ocean. They are estimated by assuming that the observations are of a phenomenon which locally has a form $F(z)e^{i(\vec{k}\cdot\vec{x}-\omega t)}$ where $|k| = 1/60$ km, $\omega = 1/10$ days and $F(z)$ has the form of the first baroclinic mode (Richman, 1972). These assumptions are consistent with the temporal and spatial scales estimated for the MODE-0 data set by Gould Schmitz and Wunsch (1974). To determine the sampling error in estimates of horizontal derivatives by a finite differencing calculation the scale $|\vec{k}|$ and horizontal separation, $\vec{\Delta x}$, of the measurements are used as follows:

$$\frac{\text{Finite Difference Estimate}}{\text{True Value}} = \frac{F(z)e^{i\vec{k}\cdot\vec{x}_0}\left(e^{\frac{i\vec{k}\cdot\vec{\Delta x}}{2}} - e^{\frac{-i\vec{k}\cdot\vec{\Delta x}}{2}}\right)}{\frac{i\vec{k}\cdot\vec{\Delta x}}{|\vec{\Delta x}|}\,F(z)e^{i\vec{k}\cdot\vec{x}_0}} =$$

$$= \frac{\sin\left(\frac{\vec{k}\cdot\vec{\Delta x}}{2}\right)}{\left(\frac{\vec{k}\cdot\vec{\Delta x}}{2}\right)}$$

The finite difference estimate is smaller by a factor $\frac{\sin\left(\frac{\vec{k}\cdot\vec{\Delta x}}{2}\right)}{(\vec{k}\cdot\vec{\Delta x}/2)}$. Likewise the finite difference estimate of a time derivative is smaller by a factor $\sin(\omega\Delta t/2)/\omega\Delta t/2$. Sampling errors in estimates of vertical derivatives or in-

tegrals are calculated by comparing the finite difference or trapezoidal rule estimate with the value obtained for the function F(z) tabulated by Richman (1972).

Theoretical errors are determined from scale analysis. They are used here only when simplifications in the calculations can be made by assuming a theoretical balance. In calculating the horizontal advection of temperature there is a great simplification if the thermal wind balance is assumed. The calculation of the horizontal advection of temperature then has a theoretical error due to the use of the thermal wind relations which are valid only within a theoretical error estimated from scale analysis. The theoretical errors are not used in testing each balance. For example, the geostrophic balance is valid only within an error based on a scale analysis of the remaining term in the horizontal momentum equations. This error is not included in testing the observed and geostrophic current differences for geostrophic balance.

The sampling errors could be eliminated if an interpolation scheme which takes into account the assumed field is used. When the known field is determined by correlation functions calculated from the observations, the interpolation scheme is that of objective analysis (Gandin, 1965). This approach is not used here because by using objective interpolation a test for balance becomes partially a test of the correlation functions and partially a test of the balance. Estimates of horizontal derivatives in objective analysis

are influcenced strongly by the behavior of the second derivatives of the correlation functions near zero separation (Batchelor, 1960) which is a region where the correlation functions calculated from observations are not well determined (Freeland, private communication). Thus, it is considered appropriate in this work to limit the effects of the assumed field to the error analysis until the correlation functions are determined more accurately.

This thesis was undertaken to investigate the extent to which basic balances of momentum, mass, heat, and vorticity for low-frequency motions can be determined directly from observations. The balances of momentum, mass and heat are established within the estimated errors and an experiment is suggested to establish the vorticity balance. But mostly, it is hoped that this work will create an optimistic attitude that careful analysis of observations can answer basic dynamical questions.

CHAPTER II

HORIZONTAL MOMENTUM BALANCE: GEOSTROPHY

INTRODUCTION

The geostrophic balance in the horizontal momentum equations has long been used by oceanographers to infer currents from measurements of density. There have been few comparisons between measured and inferred currents because of the difficulty in making current measurements. The classic comparison was done by Wüst (1924) for currents in the Florida Straits. Wüst found an average discrepancy between observed and geostrophic currents at six depths at a single station of 9 cm/sec or 18%. Wüst's comparison was cited by Sverdrup as "a convincing demonstration of the correctness of the later methods used for computing relative currents" (Sverdrup, Johnson and Fleming; 1942, 673-674). von Arx (1962) mentioned geostrophic comparisons by the International Ice Patrol, METEOR Expedition, and von Arx which showed discrepancies of about 15%. These comparisons were for high currents and used reference levels where the currents were assumed to be zero. For deep-ocean currents Swallow (1971) made comparisons between geostrophic current differences estimated from hydrostations and observed differences from float measurements. For his one detailed comparison the observed and geostrophic differences agreed within 0.9 cm/sec or 12%.

Other comparisons involving fewer measurements showed agreement within 2 to 5 cm/sec.

The geostrophic comparisons presented here significantly increase the observational evidence for a geostrophic balance in the horizontal momentum equations. In addition these comparisons, along with the tests of horizontal nondivergence in the next chapter, are tests of measurement quality. Failure of the observations to confirm geostrophy and horizontal nondivergence would be interpreted by most oceanographers as due to problems in measurements. Such a failure would limit efforts to use the observations in tests of more interesting balances, so it is important to do these tests of geostrophy and horizontal nondivergence. Another motivation for these geostrophic comparisons is to determine whether higher-order momentum balances can be attempted. Whether the deviations from geostrophic balances are larger than the estimated errors is crucial to the prediction of momentum changes. Thus, this analysis of the horizontal momentum equation presents observational evidence for the geostrophic balance, tests the quality of the observations, and determines whether higher-order momentum balances can be estimated.

THEORY

The instantaneous horizontal momentum equations may be written:

$$\frac{\partial u}{\partial t}+u\frac{\partial u}{\partial x}+v\frac{\partial u}{\partial y}+w\frac{\partial u}{\partial z}-fv+hw = -\frac{\partial p}{\rho_0 \partial x}+\nu\left(\frac{\partial^2 u}{\partial x^2}+\frac{\partial^2 u}{\partial y^2}+\frac{\partial^2 u}{\partial z^2}\right)$$

$$\frac{\partial v}{\partial t}+u\frac{\partial v}{\partial x}+v\frac{\partial v}{\partial y}+w\frac{\partial v}{\partial z}+fu = -\frac{\partial p}{\rho_0 \partial y}+\nu\left(\frac{\partial^2 v}{\partial x^2}+\frac{\partial^2 v}{\partial y^2}+\frac{\partial^2 v}{\partial z^2}\right) \qquad (2.1)$$

where (u,v,w) are velocity components in the (x,y,z)=(East, North, Upward) directions; p is pressure, ρ_0 is density of sea water; h and f are the horizontal and vertical components of the Coriolis parameter; and ν is the coefficient of kinematic viscosity. Assumptions have already been made that the sea water is a Newtonian fluid and incompressible, and that the spherical earth can be locally represented as a plane. These assumptions are reviewed by Whitham (1963) and Veronis (1973). In addition sea water is assumed to be a Boussinesq fluid so that its density is taken to be a constant in these horizontal momentum equations (Malkus, 1964).

In order to examine only long-period motions one breaks down each variable q into a time averaged, $\bar{q}$, and fluctuating, q', variables, $q = \bar{q} + q'$, and then time averages the momentum equations to obtain:

$$\frac{\partial \bar{u}}{\partial t}+\bar{u}\frac{\partial \bar{u}}{\partial x}+\bar{v}\frac{\partial \bar{u}}{\partial y}+\bar{w}\frac{\partial \bar{u}}{\partial z}-f\bar{v}+h\bar{w} =$$

$$-\frac{\partial \bar{p}}{\rho_0 \partial x}+\nu\left(\frac{\partial^2 \bar{u}}{\partial x^2}+\frac{\partial^2 \bar{u}}{\partial y^2}+\frac{\partial^2 \bar{u}}{\partial z^2}\right)-\frac{\partial}{\partial x}(\overline{u'u'})-\frac{\partial}{\partial y}(\overline{u'v'})-\frac{\partial}{\partial z}(\overline{u'w'}) \qquad (2.2)$$

$$\frac{\partial \bar{v}}{\partial t}+\bar{u}\frac{\partial \bar{v}}{\partial x}+\bar{v}\frac{\partial \bar{v}}{\partial y}+\bar{w}\frac{\partial \bar{v}}{\partial z}+f\bar{u} = \tag{2.2}$$

$$-\frac{\partial \bar{p}}{\rho_0 \partial y}+\nu\left(\frac{\partial^2 \bar{v}}{\partial x^2}+\frac{\partial^2 \bar{v}}{\partial y^2}+\frac{\partial^2 \bar{v}}{\partial z^2}\right)-\frac{\partial}{\partial x}(\overline{u'v'})-\frac{\partial}{\partial y}(\overline{v'v'})-\frac{\partial}{\partial z}(\overline{v'w'}).$$

For averaging periods greater than one day the time derivatives of the averaged current are smaller than the Coriolis accelerations:

$$\left|\frac{\partial \bar{u}}{\partial t}\right| = 0\left(\frac{\omega}{f}\right)\ |f\bar{v}|,\quad \left|\frac{\partial \bar{v}}{\partial t}\right| = 0\left(\frac{\omega}{f}\right)\ |f\bar{u}|$$

where ω is the typical frequency of the averaged ocean current variations. For horizontal length scales, L and L', larger than 10 km the advective terms are small compared with the Coriolis accelerations for typical ocean velocities ($U = 10$ cm s^{-1}, $U' = 5$ cm s^{-1}):

$$\left|\bar{u}\frac{\partial \bar{u}}{\partial x}+\bar{v}\frac{\partial \bar{u}}{\partial y}+\bar{w}\frac{\partial \bar{u}}{\partial z}\right| = 0\left(\frac{U}{fL}\right)|f\bar{v}|$$

$$\left|\bar{u}\frac{\partial \bar{v}}{\partial x}+\bar{v}\frac{\partial \bar{v}}{\partial y}+\bar{w}\frac{\partial \bar{v}}{\partial z}\right| = 0\left(\frac{U}{fL}\right)|f\bar{u}|$$

$$\left|\frac{\partial}{\partial x}(\overline{u'u'})+\frac{\partial}{\partial y}(\overline{u'v'})+\frac{\partial}{\partial z}(\overline{u'w'})\right| = 0\left(\frac{U'U'}{UfL'}\right)|f\bar{v}|$$

$$\left|\frac{\partial}{\partial x}(\overline{u'v'})+\frac{\partial}{\partial y}(\overline{v'v'})+\frac{\partial}{\partial z}(\overline{v'w'})\right| = 0\left(\frac{U'U'}{UfL'}\right)|f\bar{u}|.$$

For vertical length scales, H, larger than 1 m the viscous terms are small:

$$|\nu(\frac{\partial^2\bar{u}}{\partial x^2}+\frac{\partial^2\bar{u}}{\partial y^2}+\frac{\partial^2\bar{u}}{\partial z^2})| = 0(\frac{\nu}{fH^2},\frac{\nu}{fL^2})|f\bar{v}|$$

$$|\nu(\frac{\partial^2\bar{v}}{\partial x^2}+\frac{\partial^2\bar{v}}{\partial y^2}+\frac{\partial^2\bar{v}}{\partial z^2})| = 0(\frac{\nu}{fH^2},\frac{\nu}{fL^2})|f\bar{u}|.$$

The size of the vertical velocity, W, is assumed to be no larger than $\frac{H}{L}U$ because of the continuity equation which is discussed in Chapter III. With this assumption the horizontal Coriolis parameter term is small for H of about 1 km: $|h\bar{w}| = 0(\frac{H}{L})|f\bar{v}|$.

For these large spatial and temporal scales the horizontal momentum equations can be written:

$$\begin{aligned} -f\bar{v}(1 \pm 0(\frac{\omega}{f},\frac{U}{fL},\frac{U'U'}{UfL},\frac{\nu}{fH^2},\frac{\nu}{fL^2},\frac{H}{L})) &= -\frac{\partial\bar{p}}{\rho_0\partial x} \\ f\bar{u}(1 \pm 0(\frac{\omega}{f},\frac{U}{fL},\frac{U'U'}{UfL},\frac{\nu}{fH^2},\frac{\nu}{fL^2})) &= -\frac{\partial\bar{p}}{\rho_0\partial y}. \end{aligned} \qquad (2.3)$$

Because all other terms are much smaller than the Coriolis accelerations the horizontal pressure gradient must predominantly balance the Coriolis accelerations. This is the geostrophic balance.

It should be emphasized that the geostrophic balance holds for currents of long time scales so that ω/f is small and length scales large enough that the Rossby number, U/fL, is small. It is possible that no such motions would exist

in the ocean at these scales or that shorter scale motions would be so large that these geostrophic motions could not be observed. Many years of repeated hydrographic stations have shown, however, that there are measurable signals in the pressure field at these long periods and scales and these pressure forces should be in predominant geostrophic balance (Sverdrup, Johnson and Fleming, 1942).

The time-averaged vertical momentum balance may be written:

$$\left(\frac{\partial \bar{w}}{\partial t}+\bar{u}\frac{\partial \bar{w}}{\partial x}+\bar{v}\frac{\partial \bar{w}}{\partial y}+\bar{w}\frac{\partial \bar{w}}{\partial z}-h\bar{u}\right)=$$

$$-\frac{\partial \bar{p}}{\partial z}-\bar{\rho}g+\nu\left(\frac{\partial^2 \bar{w}}{\partial x^2}+\frac{\partial^2 \bar{w}}{\partial y^2}+\frac{\partial^2 \bar{w}}{\partial z^2}\right)-\frac{\partial}{\partial x}(\overline{u'w'})-\frac{\partial}{\partial y}(\overline{v'w'})-\frac{\partial}{\partial z}(\overline{w'w'}). \tag{2.4}$$

The gravity force is so much larger than any term involving velocity that a predominant hydrostatic balance occurs: $0 = -\frac{\partial \bar{p}}{\partial z} - \bar{\rho}g$. For a profile of density $\bar{\rho}_0(z)$ known in an average sense over the area and period of measurement, the hydrostatic pressure, $p_H = -\int g\bar{\rho}_0(z)\,dz$, can be subtracted $\bar{p}' = \bar{p} - p_H$ to leave only a pressure, $\bar{p}'$, associated with deviations from the spatially averaged hydrostatic balance, and the vertical momentum balance becomes:

$$\rho_0\left(\frac{\partial \bar{w}}{\partial t}+\bar{u}\frac{\partial \bar{w}}{\partial x}+\bar{v}\frac{\partial \bar{w}}{\partial y}+\bar{w}\frac{\partial \bar{w}}{\partial z}-h\bar{u}\right) = \tag{2.5}$$

$$-\frac{\partial \bar{p}'}{\partial z}-\bar{\rho}'g+\nu\left(\frac{\partial^2 \bar{w}}{\partial x^2}+\frac{\partial^2 \bar{w}}{\partial y^2}+\frac{\partial^2 \bar{w}}{\partial z^2}\right)-\frac{\partial}{\partial x}(\overline{u'w'})-\frac{\partial}{\partial y}(\overline{v'w'})-\frac{\partial}{\partial z}(\overline{w'w'})$$

where $\bar{\rho}' = \bar{\rho} - \bar{\rho}_0(z)$. From the geostrophic balance in the horizontal momentum equations the dynamically important pressure, $\bar{p}'$, must have size $\rho_0 FUL$. For large time and space scales even $\bar{p}'$ is in local hydrostatic balance:

$$\frac{\partial \bar{p}'}{\partial z}\left(1 + 0\left(\frac{H}{L}, \frac{H'^2}{L'^2}, \frac{\nu}{fL^2}\right)\right) = -\bar{\rho}' g. \tag{2.6}$$

From the geostrophic and hydrostatic balances (equations 2.3 and 2.6) the thermal wind equations can then be obtained by eliminating pressure:

$$\begin{aligned} -\rho_0 f\frac{\partial v}{\partial z} &= g\frac{\partial \rho'}{\partial x}(1 \pm 0(\varepsilon)) \\ \rho_0 f\frac{\partial u}{\partial z} &= g\frac{\partial \rho'}{\partial y}(1 \pm 0(\varepsilon)) \end{aligned} \tag{2.7}$$

where ε is the largest of $\left(\frac{\omega}{f}, \frac{U}{fL}, \frac{U'U'}{UfL}, \frac{\nu}{fH^2}, \frac{\nu}{fL^2}, \frac{H}{L}, \frac{H'^2}{L'^2}\right)$ and where the bars are removed for convenience in future usage. In the MODE region a strong relationship exists between temperature and salinity so that $S = S(T)$ (Iselin, 1936) and density, $\bar{\rho}'$ which is a function of salinity and temperature may be considered to be a function of temperature alone:
$\bar{\rho}'(T,S) = \bar{\rho}'(T, S(T)) = \bar{\rho}'(T)$ and $d\bar{\rho}' = \frac{\partial \bar{\rho}'}{\partial T}dT + \frac{\partial \bar{\rho}'}{\partial S}dS = \left(\frac{\partial \bar{\rho}'}{\partial T} + \frac{\partial \bar{\rho}'}{\partial S}\frac{dS}{dT}\right)dT = -\alpha dT$. This relationship allows the thermal wind equations to be written in terms of temperature:

$$\rho_0 f\frac{\partial v}{\partial z} = g\alpha \frac{\partial T}{\partial x} (1 \pm 0(\varepsilon))$$

$$-\rho_0 f\frac{\partial u}{\partial z} = g\alpha \frac{\partial T}{\partial y} (1 \pm 0(\varepsilon)) \qquad (2.8)$$

These thermal wind equations can be integrated vertically to yield:

$$V_n(z_1) - V_n(z_2) = \frac{g}{\rho_0 f} \int_{z_2}^{z_1} \alpha \frac{\partial T}{\partial s} dz \qquad (2.9)$$

where $\vec{n}$ and $\vec{s}$ are orthogonal unit vectors with $\vec{s}$ $\pi/2$ radians clockwise from $\vec{n}$ in the Northern Hemisphere.

DATA AND METHODS

Because most temperature recorders worked during MODE-1 while many current meters malfunctioned, two types of calculations are done. First, thermal wind correlations in accordance with equation 2.8 between time series of horizontal temperature gradient estimates and vertical shear of horizontal current estimates are done. These calculations require only one pair of working current meters on a single mooring from which a time series of vertical shear of horizontal current can be correlated with many time series of horizontal temperature gradient. Secondly, geostrophic comparisons in accordance with equation 2.9 are done when there were two moorings with working current meters at two depths. These comparisons allow tests of

geostrophic balance within estimated errors to be made.

The measurements used were recorded on moorings at depths shallower than 1500 m as part of the MODE-1 field program (Figure 1.1). Each mooring had current meters also measuring temperature at nominal depths of 420, 720 and 1420 m and pressure-temperature recorders at nominal depths of 520 and 920 m. Wunsch, Hogg and Richman (1974) examined the pressure records and found variations of ±40 m in the depths of instruments nominally at the same level. They also found that instrument depth varied daily because moorings tilt more or less depending on currents.

In order to make accurate estimates of horizontal temperature gradients the temperature at each instrument is changed to represent the temperature at standard pressures (420, 520, 720 and 920 dbar). The nominal 1420 m temperatures are not corrected because of uncertainties in the mean vertical temperature gradient and in the T/S properties of the water due to intrusions of Mediterranean Water at this depth (Hayes, 1975). The temperature change is accomplished in two steps. First, the temperature is corrected to the average pressure of the instrument, $\bar{p}_i$, by adding the pressure difference multiplied by the mean temperature gradient for daily values of pressure, p_i, and temperature, T: $T(\bar{p}_i) = T(p_i) + (\bar{p}_i - p_i) \frac{\overline{\partial T}}{\partial p}$. Pressures were measured only at 520 and 920 m nominal depths. The pressure at 420 m nominal depth is taken to be 100 dbar

less than the pressure at 520 m. The pressure at 720 m nominal depth is taken to be the average of the pressures at 520 and 920 m. The mean vertical gradient of temperature is obtained from a horizontal average of nine CTD stations (Millard and Bryden, 1973). Secondly, a constant temperature, ΔT_i, obtained from the average CTD station is added to or subtracted from the temperature at the actual average instrument pressure to bring the temperature to a value representative of the average pressure for all moorings, $\langle p \rangle$: $T(\langle p \rangle) = T(\bar{p}_i) + \Delta T_i$. Due to uncertainties in using values from the average CTD station at a particular place, it is estimated that this procedure could introduce errors in temperature equal to 10% of the total temperature correction.

Horizontal temperature gradients are estimated by differencing corrected temperatures between moorings and dividing by the mooring separation

$$\frac{\partial T}{\partial s} = \frac{T_j(\langle p \rangle) - T_i(\langle p \rangle)}{\Delta s_{ij}} = \frac{\Delta T_{ij}}{\Delta s_{ij}}$$

where Δs_{ij} is the distance between moorings i and j. The error in these estimates is $\frac{.032°C}{\Delta s_{ij}}$ due to measurement errors and $.10 \frac{\Delta p_{ij}}{\Delta s_{ij}} \overline{\frac{\partial T}{\partial p}}$ where Δp_{ij} is the difference in average pressures on moorings i and j due to the temperature correction procedure. The estimates may be smaller than the true values by a factor

$\frac{\sin(\frac{\Delta s_{ij}}{120\ km})}{(\Delta s_{ij}/120\ km)}$ due to sampling errors. Vertical shears of horizontal velocity are estimated by differencing velocities at separate depths on the same mooring and dividing by the vertical separation. Only velocities normal to the line joining the two moorings are used:

$$\frac{\partial v_n}{\partial z} = \frac{\vec{\Delta V} \times \vec{\Delta s}_{ij}/|\vec{\Delta s}_{ij}|}{\Delta z}.$$

Errors in these estimates are $\frac{\sqrt{2} \times 0.45\ cm\ s^{-1}}{\Delta z}$ due to the measurement errors. The estimates also have a sampling error depending on the vertical separation calculated from comparison with the theoretical first baroclinic mode. Thermal wind correlations are calculated from these estimates of horizontal temperature gradient and vertical shear of horizontal current using the shears on MODE-1 moorings 2, 3, 6, 7 and 10. Correlations are calculated as a function of time lag in days up to a maximum lag of one-sixth the common length of the two time series for moorings separated by less than 120 km. The maximum correlation coefficient is chosen and tested against a null hypothesis of no correlation at a 99% confidence level (Pearson and Hartley, 1970). Periods of good current measurements on moorings 1 and 8 were so short that correlations involving vertical shears on these moorings are not done. I feel that the currents at 420 m on mooring 4

had questionable direction measurements so correlations involving shears on mooring 4 are not done.

To obtain the geostrophic current difference,

$$\frac{g}{\rho_0 f} \int_{z_2}^{z_2+\Delta H} \alpha \frac{\partial T}{\partial s}\, dz,$$

for geostrophic comparisons according to equation 2.9 the horizontal temperature gradients must be converted to density gradients and integrated vertically. The accuracy with which density can be predicted from temperature depends on the tightness of the T/S relationship. From 38 CTD stations during MODE-1 (Fofonoff, 1973) it is estimated that variations in density for constant temperature equal $\pm .2 \times 10^{-4}$ gm/cm^3 in the main thermocline. By assuming this variation represents two standard deviations, the error in converting temperature to density becomes $\pm .1 \times 10^{-4}$ gm/cm^3. Vertical integration results in an error in geostrophic current difference of

$$\frac{g}{\rho_0 f} \frac{\sqrt{2}\ .1 \times 10^{-4}}{\Delta s_{ij}} \Delta H \text{ or about 2 cm/sec for } \Delta s_{ij} = 100 \text{ km}$$

and $\Delta H = 1$ km. There is also an error of 5% in estimates of the magnitude of $\alpha = -\frac{d\rho}{dT}$ determined from the mean CTD station (Millard and Bryden, 1973).

By assuming the errors in measurement of temperature are random and normal, the error in geostrophic current dif-

ference due to measurement errors is $\frac{1}{\sqrt{N}} \frac{g\alpha}{\rho_0 f} \frac{.032°C}{\Delta s_{ij}} \Delta H$ or .20 cm/sec for Δs_{ij} = 100 km, ΔH = 1 km, and N = 5 where N is the number of temperature measurements on each mooring. The errors due to temperature correction are assumed to be constant during integration so the error in geostrophic current difference is $.10 \frac{g\alpha}{\rho_0 f} \frac{\overline{\partial T}}{\partial p} \frac{\Delta p_{ij}}{\Delta s_{ij}} \Delta H$. The sampling error due to the trapezoidal integration procedure varies with the depth interval over which the horizontal temperature gradients are integrated. Comparisons with first baroclinic mode integrations (Richman, 1972) show that trapezoidal integration estimates of geostrophic current difference are 6% larger than the baroclinic mode value for the depth interval 1420 m to 720 m; 7% larger for the interval 1420 m to 420 m; and 9% larger for the interval 720 m to 420 m. Thus, there are errors in geostrophic current differences due to the conversion of temperature to density, uncertainties in the magnitude of α, measurement errors in temperature, the temperature correction procedure, and trapezoidal integration.

Observed current differences are estimated by differencing observed velocities at two depths: $\Delta V_n = \vec{\Delta V} \times \Delta s_{ij} / |\Delta s_{ij}|$. To make geostrophic comparisons the observed current differences are averaged for two moorings. The error in this average current difference is .45 cm/sec due to measurement errors. In addition there is a sampling error so that the average current difference may be smaller

than the theoretical value by a factor $\frac{(k\Delta x)}{2} \Big/ \tan\frac{(k\Delta x)}{2}$. Geostrophic comparisons are made only when the velocity differences at each mooring are of the same sign because differences of opposite signs indicate a maximum or minimum in temperature which limits the accuracy of the horizontal temperature gradients. Four-day averaged geostrophic and observed current differences with their errors are compared for mooring pairs 1-8, 2-6, 2-7, 6-7, 2-3, and 3-6.

RESULTS AND DISCUSSION

The percentage of significant thermal wind correlations depends on the mooring for which the velocity shears are estimated and on the horizontal mooring separation over which the horizontal temperature gradients are estimated (Table 2.1). The percentage of correlations significant at a 99% confidence level is smallest for mooring 2 (Table 2.1a). Some of the records on mooring 2 were interrupted when it was struck by a towfish. This hit stretched the mooring so that the average instrument depth decreased by 40 m at the top of the mooring. Temperatures are corrected to the same average pressures separately for time periods before and after the hit but the separate corrections may create a discontinuity in temperature time series and hence a discontinuity in horizontal temperature gradient time series involving mooring 2. A discontinuity

Table 2.1a

Mooring	Number of Correlations	Number of Significant Correlations	% Significant Correlations
2	73	27	37
3	19	17	89
6	64	47	73
7	28	21	75
10	6	3	50

Table 2.1b

Horizontal Separation	Number of Correlations	Number of Significant Correlations	% Significant Correlations
51-63 km	20	19	95
87-95 km	13	12	92
99-104 km	28	22	79
107-112 km	19	13	68

Table 2.1 Results of thermal wind correlations from MODE-1 measurements. The number and percentage of significantly non-zero correlations at a 99% confidence level between vertical shear of current and horizontal temperature gradient are given as a function of: a) MODE-1 mooring number; b) horizontal separation between moorings. For b) correlations involving horizontal temperature gradients using temperatures at mooring 2 or at 1420 m nominal depth are excluded.

would reduce correlations so it is not surprising that the percentage of significant correlations is low for mooring 2. Mooring 10 also had a low percentage of significant correlations (Table 2.1a). All correlations using mooring 10 involve temperatures at 1420 m depth where density is not related to temperature as strongly as at shallower depths so the low percentage is not unexpected.

Excluding correlations involving mooring 2 and temperatures at 1420 m depth, which are not expected to be significant, results in 82% (63 of 77) of the thermal wind correlations being significantly nonzero at a 99% confidence level. The percentage of significant correlations decreases as the mooring separation increases but even at separations of 110 km 68% of the correlations are significantly nonzero at a 99% confidence level (Table 2.1b). The decrease is attributed to larger sampling errors at the larger mooring separations.

Geostrophic comparisons are made for daily values of observed and geostrophic current differences (Figure 2.1). These daily values have a correlation coefficient of 0.92, significantly nonzero at a 99% confidence level (Pearson and Hartley, 1970). A linear regression gives a slope not significantly different from 1 and an intercept not significantly different from 0 at a 95% confidence level (using methods outlined in Fofonoff and Bryden, 1975).

Geostrophic comparisons are made for four-day estimates of observed and geostrophic current differences

Figure 2.1. Daily observed current differences plotted against estimates of geostrophic current difference for all MODE-1 geostrophic comparisons. The correlation coefficient is calculated to be 0.92. The line of slope 1 and intercept 0 is the line of geostrophic agreement. Typical errors are indicated.

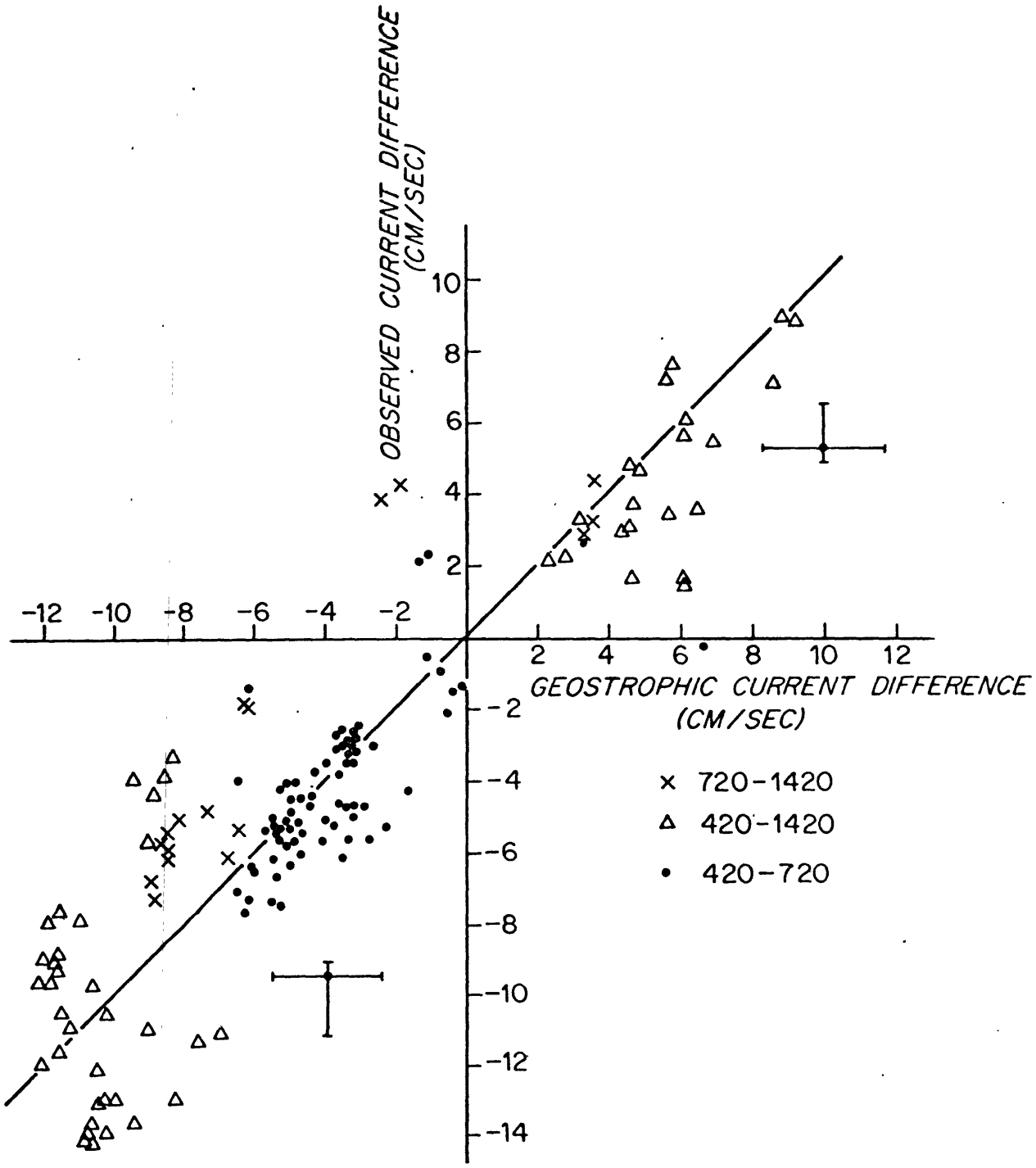
OBSERVED CURRENT DIFFERENCE (CM/SEC)
GEOSTROPHIC CURRENT DIFFERENCE (CM/SEC)
10
8
6
4
2
-2
-4
-6
-8
-10
-12
-14
-12
-10
-8
-6
-4
-2
2
4
6
8
10
12
× 720-1420
△ 420-1420
• 420-720

(Table 2.2). All but two of the thirty-two comparisons agree within estimated two standard deviation errors and all comparisons agree within three standard deviation errors. Because of the uncertainty in the error estimates it is reasonable to use three standard deviations as error bounds. Within these error bounds the observed and geostrophic current differences are in geostrophic balance. For four-day estimates, the geostrophic current difference accounts for 92% of the variance in the observed current differences. The standard deviation of the discrepancy between observed and geostrophic differences is 1.9 cm/sec, which is 26% of the standard deviation of the observed current differences.

A geostrophic comparison is done with the longest time series of estimates of observed and geostrophic current differences for the mooring pair 3 and 6 (Figure 2.2 taken from Bryden, 1974). The average discrepancy between observed and geostrophic differences is 0.01 cm/sec while the standard deviation of the four-day averaged discrepancies is 1.01 cm/sec or 20% of the average differences.

Using floats, CTD stations and moored temperature measurements during MODE-1 Swallow (1975) found agreement between observed and geostrophic differences for one four-day period over the depth interval 500 to 1500 m within 0.5 cm/sec and over the depth inverval 1600 m to 2900 m within 0.13 cm/sec both of which were less

Table 2.2

Geostrophic comparisons: a) for vertical differences of current between 720 m and 1420 m nominal depths; b) for vertical differences between 420 m and 1420 m; c) for vertical differences between 420 m and 720 m. Four-day values of current and temperature are used. The average observed current difference is the average of observed current differences at the two moorings. The geostrophic current difference is the vertical integral of horizontal temperature gradients according to equation 2.9. The errors represent estimated one standard deviation errors. The error ranges are not symmetric about the estimate because sampling errors result in a constant offset toward larger or smaller values. The sampling error in average observed current difference depends on whether the line joining two moorings is parallel or perpendicular to $\vec{k}$. For this reason tests of geostrophic agreement are done for a range of observed differences from the estimate to a smaller value due to sampling errors calculated for separations parallel to $\vec{k}$. One asterisk (*) denotes a discrepancy of one to two standard deviations from geostrophic agreement. Two asterisks (**) denote discrepancies of two to three standard deviations.

Table 2.2a

Current Differences Between 720 m and 1420 m Depths

Average Observed Current Difference cm/sec	Geostrophic Current Difference cm/sec	Range in Observed Current Difference cm/sec	Range in Geostrophic Current Difference cm/sec
Moorings 1 and 8			
3.21	3.27	3.21 - .45 4.22 + .45	3.08 ± 1.48
Moorings 2 and 6			
-5.32	-7.65	-5.32 + .45 -7.49 - .45	-7.22 ± 1.42
-6.67	-8.72	-6.67 + .45 -9.39 - .45	-8.23 ± 1.44

Table 2.2b

Current Differences Between 420 m and 1420 m Depths

	Average Observed Current Difference cm/sec	Geostrophic Current Difference cm/sec	Range in Observed Current Difference cm/sec	Range in Geostrophic Current Difference cm/sec
Moorings 1 and 8				
	3.67	4.53	3.67 - .45 4.83 + .45	4.23 ± 2.04
Moorings 2 and 6				
	-6.08	-9.67	-6.08 + .45 -8.56 - .45	-9.04 ± 1.98
	-8.48	-11.25	-8.48 + .45 -11.94 - .45	-10.51 ± 2.00
	-9.96	-11.94	-9.96 + .45 -14.03 - .45	-11.16 ± 2.01
	-8.22	-11.84	-8.22 + .45 -11.58 - .45	-11.07 ± 2.01
Moorings 2 and 7				
*	-14.05	-10.69	-14.05 + .45 -15.44 - .45	-9.99 ± 3.70
	-13.14	-10.35	-13.14 + .45 -14.44 - .45	-9.67 ± 3.70
	-11.38	-11.38	-11.38 + .45 -12.51 - .45	-10.64 ± 3.70
	-11.03	-8.46	-11.03 + .45 -12.12 - .45	-7.91 ± 3.69
Moorings 6 and 7				
	1.52	3.46	1.52 - .45 1.95 + .45	3.23 ± 2.08
*	2.58	6.09	2.58 - .45 3.31 + .45	5.69 ± 2.10
	6.66	5.85	6.66 - .45 8.54 + .45	5.47 ± 2.10
	6.35	8.54	6.35 - .45 8.14 + .45	7.98 ± 2.12

Table 2.2c

Current Differences Between 420 m and 720 m Depths

	Average Observed Current Difference cm/sec	Geostrophic Current Difference cm/sec	Range in Observed Current Difference cm/sec	Range in Geostrophic Current Difference cm/sec
Moorings 2 and 3				
**	1.13	-1.03	1.13 - .45 1.38 + .45	-0.94 ± .77
*	-1.66	-0.31	-1.66 + .45 -2.02 - .45	-0.28 ± .77
Moorings 2 and 6				
**	-5.23	-3.34	-5.23 + .45 -7.37 - .45	-3.06 ± .63
	-3.16	-3.60	-3.16 + .45 -4.45 - .45	-3.30 ± .64
	-3.29	-3.22	-3.29 + .45 -4.63 - .45	-2.95 ± .63
	-2.92	-3.22	-2.92 + .45 -4.11 - .45	-2.95 ± .63
Moorings 3 and 6				
*	-5.76	-4.33	-5.76 + .45 -6.33 - .45	-3.97 ± 1.00
	-4.64	-5.01	-4.64 + .45 -5.10 - .45	-4.60 ± 1.00
	-5.21	-5.12	-5.21 + .45 -5.73 - .45	-4.70 ± 1.00
	-5.31	-5.21	-5.31 + .45 -5.84 - .45	-4.78 ± 1.00
	-4.60	-4.58	-4.60 + .45 -5.05 - .45	-4.20 ± 1.00
	-5.02	-5.55	-5.02 + .45 -5.52 - .45	-5.09 ± 1.01
*	-7.12	-6.24	-7.12 + .45 -7.84 - .45	-5.72 ± 1.02
*	-6.94	-5.29	-6.94 + .45 -7.63 - .45	-4.85 ± 1.00
	-3.87	-5.74	-3.87 + .45 -4.25 - .45	-5.27 ± 1.01
	-2.88	-3.71	-2.88 + .45 -3.16 - .45	-3.40 ± 0.99

Figure 2.2 Comparison of observed and geostrophic current differences for MODE-1 moorings 3 and 6. Observed current differences, Δv_n (——), and geostrophic current differences, $\frac{g}{\rho_0 f} \int_{-720}^{-420} \alpha \frac{\partial T}{\partial s} dz$ (----), are for the depth interval 420 to 720 m.

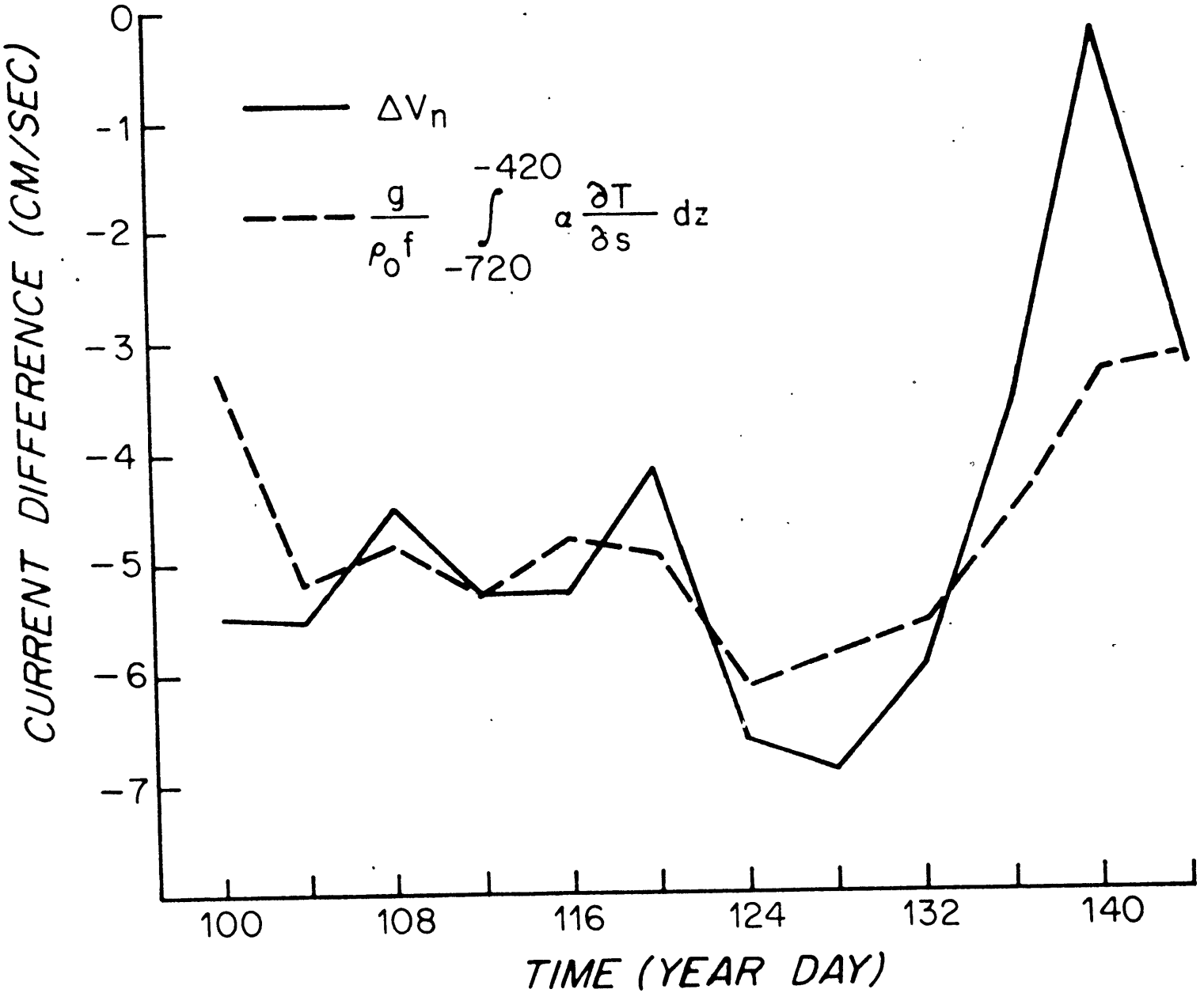
0
-1
-2
-3
-4
-5
-6
-7
CURRENT DIFFERENCE (CM/SEC)
ΔV_n
$\frac{g}{\rho_0 f} \int_{-720}^{-420} \alpha \frac{\partial T}{\partial s} dz$
100
108
116
124
132
140
TIME (YEAR DAY)

than estimated errors. Using current meters on mooring 3 and STD stations Horton and Sturges (1975) compared observed and geostrophic current differences between 420 and 720 m and 420 and 2940 m depths. The average discrepancy over 70 days between observed and geostrophic differences was .9 cm/sec for the 420 - 720 m depth interval and .5 cm/sec for the 420 - 2940 m interval.

That the observed and geostrophic current differences presented here and by Swallow balance within estimated errors suggests that these errors must be reduced before higher-order momentum balances can be attempted. It is interesting to determine whether the errors in observed and geostrophic current differences and in estimates of horizontal advection of momentum are small enough that local time changes of momentum could be predicted from estimates of advection of momentum and deviations from geostrophic balance. For motions of amplitude 10 cm/sec, frequency 1/10 days and horizontal wavenumber 1/60 km similar to those observed during MODE-0 (Gould, Schmitz and Wunsch, 1974), local accelerations ($\frac{\partial u}{\partial t}$ and $\frac{\partial v}{\partial t}$) are of size $1 \frac{cm}{sec}$/day.

Estimates of horizontal advection of momentum with errors smaller than $1 \frac{cm}{sec}$/day can be made in higher order momentum balances. Use of horizontal nondivergence (equation 3.3) allows a simplification in the estimation of horizontal advection of momentum to be made:

$$u\frac{\partial u}{\partial x} + v\frac{\partial u}{\partial y} = u(-\frac{\partial v}{\partial y})(1\pm 0(\delta)) + v\frac{\partial u}{\partial y} = -S^2\frac{\partial \theta}{\partial y}\pm 0(\delta)u\frac{\partial u}{\partial x}$$

$$u\frac{\partial v}{\partial x} + v\frac{\partial v}{\partial y} = u\frac{\partial v}{\partial x} + v(-\frac{\partial u}{\partial x})(1\pm 0(\delta)) = S^2\frac{\partial \theta}{\partial x}\pm 0(\delta)v\frac{\partial v}{\partial y} \qquad (2.10)$$

where a transformation to notation with horizontal velocity described by speed, S, and direction, θ, measured positively counterclockwise from East is used and δ is defined after equation 3.3. For horizontal separations of 50 km and speed 10 cm/sec, the measurement error in speed results in an error of 10% and the measurement error in current direction in an error of $\pm.13\frac{cm}{sec}$/day in the estimates of horizontal advection of momentum. The additional error due to the assumption of horizontal non-divergence should be only of order 5% of the individual non-linear terms. Provided the advection of momentum is of size 1 $\frac{cm}{sec}$/day and $\vec{u}$ and $\vec{\nabla}u$ and $\vec{u}$ and $\vec{\nabla}v$ are not within 10° of perpendicularity, these estimates of horizontal advection should be larger than the errors. The representation of horizontal advection of momentum in equation 2.10 also will be useful in exploring the vorticity balance (Chapter V).

Estimates of deviations from geostrophic balance cannot be made with errors smaller than $1\frac{cm}{sec}$/day. In order to estimate deviations from geostrophic balance as small as $1\frac{cm}{sec}$/day it is necessary to reduce errors in observed and geostrophic current differences

to less than 0.2 cm/sec, which is less than half the measurement error in velocity determined from IWEX comparisons. Measurement and sampling errors can be reduced by obtaining measurements from many instruments, but the most difficult error to eliminate is in the estimation of density. For a calculation over 300 m vertically and 50 km horizontally the error in density must be reduced to 2 ppm to achieve an error in geostrophic current difference of 0.2 cm/sec. For carefully calibrated CTD stations over a 10 km square area (Millard, private communication) the variations in density at constant temperature are ±4 ppm even in the main thermocline where the T/S relationship is strongest. Thus, the deviations from geostrophic balance cannot be calculated from moored measurements with accuracy sufficient to estimate local time changes of momentum in the MODE region so that higher-order momentum balances should not be attempted.

CONCLUSIONS

Thermal wind correlations and geostrophic comparisons give agreement with a geostrophic balance within estimated errors. Eighty-two percent of the correlations are significantly nonzero at a 99% confidence level. Most of the nonsignificant correlations occur for larger spatial separations where the sampling errors are larger. All thirty-two geostrophic comparisons give agreement with geostrophic balance within estimated three standard deviation errors.

A geostrophic balance as the lowest-order horizontal momentum balance is indicated by these results.

Prediction of local time changes of momentum from estimates of deviations from geostrophy and horizontal advection of momentum is not possible because of the small error (±.2 cm/sec) required in estimates of geostrophic and observed current differences. At present instrumental errors cause errors larger than .2 cm/sec, but the prohibitive factor for future work is the small error in density (±2 ppm) required to estimate geostrophic current differences within .2 cm/sec.

CHAPTER III

MASS BALANCE: HORIZONTAL NONDIVERGENCE

INTRODUCTION

The geostrophic balance in the horizontal momentum equations constrains the mass balance for large-scale, low-frequency currents to be nearly horizontally nondivergent. Tests for horizontal nondivergence are possible from a small array of velocity measurements. Small measurement errors in velocity, however, can cause the observed velocity field to appear divergent especially for short horizontal separations such as those used by Shonting (1969). Tests for horizontal nondivergence are carried out here to provide an observational basis for this balance. As with geostrophy, horizontal nondivergence is so well defined on theoretical grounds that most oceanographers would attribute its contradiction to measurement errors in velocity. These calculations then are also tests of the measurements and, in particular, tests of how accurately estimates of horizontal derivatives of velocity can be made from velocity measurements.

Another motivation for this work is to obtain accurate estimates of horizontal divergence for use in vorticity balance calculations (Chapter V). Meteorologists have debated the feasibility of estimating horizontal divergence and vertical velocity from wind measurements for a long

time (Panofsky, 1951; Fleagle, 1972). Because of the smallness of horizontal divergence compared with horizontal derivatives of velocity, small errors in estimates of horizontal derivatives become overwhelming errors in horizontal divergence. Estimates of horizontal derivatives and their expected errors for ocean measurements then determine the feasibility of estimating horizontal divergence directly in the ocean.

THEORY

The conservation of mass can be written:

$$\frac{\partial \rho}{\partial t} + u\frac{\partial \rho}{\partial x} + v\frac{\partial \rho}{\partial y} + w\frac{\partial \rho}{\partial z} = -\rho\left(\frac{\partial u}{\partial x} + \frac{\partial v}{\partial y} + \frac{\partial w}{\partial z}\right) \qquad (3.1)$$

Because the density of sea water, ρ, can be written as a sum of a constant, ρ_0, and a variable part, ρ': $\rho=\rho_0+\rho'$ with ρ' much smaller than ρ_0, the conservation of mass reduces to:

$$\left(\frac{\partial u}{\partial x} + \frac{\partial v}{\partial y} + \frac{\partial w}{\partial z}\right) = 0 \quad (\rho'/\rho_0)\left|\frac{\partial u}{\partial x}\right| \qquad (3.2)$$

providing only that the time scales considered are long enough that sound waves can be neglected. This is a statement that sea water is essentially incompressible. Batchelor (1967, p. 167-169) has reviewed these assumptions. Thus, the divergence of the velocity field, $\frac{\partial u}{\partial x} + \frac{\partial v}{\partial y} + \frac{\partial w}{\partial z}$, is zero to lowest order.

Elimination of pressure from the geostrophic balance (Equations 2.3) shows that the horizontal divergence, $\frac{\partial u}{\partial x} + \frac{\partial v}{\partial y}$, also should be zero to lowest order for nearly geostrophic motions:

$$\frac{\partial u}{\partial x} + \frac{\partial v}{\partial y} = 0(\delta) \left|\frac{\partial u}{\partial x}\right| \tag{3.3}$$

where δ is the largest of $(\frac{\omega}{f}, \frac{U}{fL}, \frac{U'}{fL}, \frac{\nu}{fH^2}, \frac{\nu}{fL^2}, \frac{H}{L}, \frac{L}{R})$ and R is the radius of the earth. This statement indicates that values $\frac{\partial u}{\partial x}$ and $\frac{\partial v}{\partial y}$ should be of opposite signs and almost the same magnitude so that their sum is small compared to their individual magnitudes. Their sum is an estimate of $-\frac{\partial w}{\partial z}$ according to Equation 3.2.

DATA AND METHODS

Measurements of velocity and temperature recorded by four current meters at a nominal depth of 1500 m on subsurface moorings deployed as part of MODE-0 Array 1 (Figure 1.2, Table 3.1) are considered. The four current meters recorded data during a common time period of 52 days. Only the current meters on moorings 1 and 3 (Figure 1.2) recorded temperature. Other measurements on nearby surface moorings are not considered because of possible contamination of velocity measurements by surface motions of the buoys (Gould and Sambuco, 1975).

Estimates of horizontal derivatives are made by differencing velocities along diagonals of the array to ob-

Table 3.1

Mooring	Depth of current meter	W.H.O.I. Data Number	Position	Variables recorded
1	1522 m	4091	28 01.50N 70 06.8 W	Current, Temperature
2	1503 m	4081	27 49.00N 70 08.8 W	Current
3	1502 m	4121	28 00.2 N 69 41.5 W	Current, Temperature
4	1504 m	4101	28 21.5 N 69 41.5 W	Current

Table 3.1. MODE-0 Array 1 data used in tests for horizontal nondivergence.

tain estimates of $\frac{\partial u}{\partial \eta}$, $\frac{\partial v}{\partial \eta}$, $\frac{\partial u}{\partial \tau}$, $\frac{\partial v}{\partial \tau}$ where $\vec{\tau}$ and $\vec{\eta}$ are the axes of the skewed coordinate system determined by the diagonals. The coordinate system then is changed to a rectangular system, (x,y) = (East, North), to obtain estimates of $\frac{\partial u}{\partial x}$, $\frac{\partial u}{\partial y}$, $\frac{\partial v}{\partial x}$, $\frac{\partial v}{\partial y}$. Based on horizontal scales for the array of 41 km in the x-direction and 60 km in the y-direction the errors in these estimates of horizontal derivatives of velocity are $\pm .15 \times 10^{-6}$ sec^{-1} due to measurement errors in velocity. Because of sampling errors estimates of $\frac{\partial u}{\partial x}$, $\frac{\partial v}{\partial x}$ may be small by 2% and estimates of $\frac{\partial u}{\partial y}$, $\frac{\partial v}{\partial y}$ small by 4%.

By the divergence theorem estimates of horizontal divergence obtained by integrating the velocity normal to the line segment joining each pair of moorings around the array and dividing by the area enclosed, $\frac{\partial u}{\partial x} + \frac{\partial v}{\partial y} = \frac{\oint \vec{u} \cdot d\vec{n}}{\text{Area}}$, are theoretically the same as estimates of horizontal divergence obtained from estimates of horizontal derivatives made above. Numerically, the values of horizontal divergence by the two methods are identical for a three- or four-mooring array provided the normal velocity is obtained by averaging the normal velocities at the two moorings determining the line segment. Estimates of vorticity, $\frac{\partial v}{\partial x} - \frac{\partial u}{\partial y} = \zeta$, obtained by application of Stokes Theorem, $\frac{\partial v}{\partial x} - \frac{\partial u}{\partial y} = \frac{\oint \vec{u} \cdot d\vec{s}}{\text{Area}}$, are also numerically identical to those obtained from estimates of horizontal derivatives above. Errors in estimates of horizontal divergence and vorticity are $\pm .22 \times 10^{-6}$ sec^{-1} due to measurement errors. Due to

sampling errors there may be errors in horizontal divergence of $+2\% \frac{\partial u}{\partial x} + 4\% \frac{\partial v}{\partial y}$ and in vorticity of $+2\% \frac{\partial v}{\partial x} - 4\% \frac{\partial u}{\partial y}$.

Because these errors in horizontal divergence may be larger than the expected value of the divergence, indirect estimates of horizontal divergence are made from an inviscid, linear vorticity balance, $\frac{\partial}{\partial t}(\frac{\partial v}{\partial x} - \frac{\partial u}{\partial y}) + \beta v = f \frac{\partial w}{\partial z}$ where β is the northward derivative of the Coriolis parameter, and from a non-diffusive, linear heat balance, $\frac{\partial T}{\partial t} + w\frac{\partial \overline{T}}{\partial z} = 0$. Because of the neglect of nonlinear terms which are important in these balances by scale analysis (equations 4.2, 5.1), these indirect estimates should be regarded as estimates of the order of magnitude only. In Chapter IV it is shown that for IWEX measurements the local temperature change is balanced by horizontal advection of temperature so that vertical velocities are smaller than predicted by a linear heat balance. Thus, because of the neglect of horizontal advection, these indirect estimates of horizontal divergence may be too large. If these indirect estimates are smaller than the errors in the direct estimates, the direct estimates of horizontal divergence do not represent true horizontal divergence because they are dominated by errors.

The errors in the indirect estimates of horizontal divergence magnitude are much smaller than the errors in direct estimates. In the vorticity balance, time derivatives of vorticity are estimated from differences of five-day averaged values of vorticity and estimates of northward velocity are obtained by averaging northward velocities for

the four current meters. Errors in estimates of horizontal divergence, $-\frac{\partial w}{\partial z} = -\left(\frac{\partial}{\partial t}\left(\frac{\partial v}{\partial x} - \frac{\partial u}{\partial y}\right) + \beta v\right)/f$, are 1.1×10^{-8} sec^{-1} due to measurement and sampling errors for typical velocities of amplitude 10 cm/sec and horizontal scale 60 km.

In the heat balance, time derivatives of temperature are estimated from differences of five-day averaged temperatures and the vertical gradient of temperature is determined from a mean CTD station (Millard and Bryden, 1973). To obtain an estimate of horizontal divergence it is assumed that the vertical velocity decreases linearly from its value at 1500 m depth to zero at the ocean bottom, $\frac{\partial w}{\partial z} = \left(-\frac{\partial T}{\partial t}/\overline{\frac{\partial T}{\partial z}}\right)/3500$ m. This assumption is suggested by the fact that the vertical profile of horizontal velocity from measurements in this region is similar to a theoretical first baroclinic mode (Gould, Schmitz and Wunsch, 1974) which has a nearly linear decrease of vertical velocity from 1500 m to the bottom (Richman, 1972). The sampling errors are large for this estimate of horizontal divergence; the estimate is three times larger than the value obtained for a first baroclinic mode. For isotherm displacements of 30 m over 10 day time scales, these estimates are of magnitude 1×10^{-8} sec^{-1} and have errors of 1×10^{-8} sec^{-1}.

Thus, errors in indirect estimates of the order of magnitude of horizontal divergence are 1×10^{-8} sec^{-1} which are much smaller than the errors in direct estimates of $.22 \times 10^{-6}$ sec^{-1}. These indirect estimates then can be

used to determine whether direct estimates of horizontal divergence are too large due to their measurement and sampling errors.

RESULTS AND DISCUSSION

Daily estimates of $\frac{\partial u}{\partial x}$ and $\frac{\partial v}{\partial y}$ (Figure 3.1) have a correlation coefficient of -0.93 which is significantly different from zero at a 99% confidence level. Four-day averaged estimates of $\frac{\partial u}{\partial x}$ and $\frac{\partial v}{\partial y}$ are examined for horizontal nondivergence (Table 3.2). Nine of the twelve comparisons yield horizontal nondivergence within one standard deviation error of $.22 \times 10^{-6}$ sec^{-1}, two within one to two standard deviations, and one comparison within two to three standard deviations. This last comparison occurs during a time period when estimates of $\frac{\partial u}{\partial x}$ and $\frac{\partial v}{\partial y}$ are changing rapidly. Thus, within expected errors the velocity field is horizontally nondivergent.

That estimates of $\frac{\partial u}{\partial x}$ and $\frac{\partial v}{\partial y}$ are horizontally nondivergent within expected errors gives confidence that estimates of horizontal derivatives of velocity (Figure 3.2) are accurate within standard deviation errors of $\pm.15 \times 10^{-6}$ sec^{-1}. In particular, estimates of vorticity should be accurate within $\pm.15 \times 10^{-6}$ sec^{-1} $\times \sqrt{2} =$ $\pm.22 \times 10^{-6}$ sec^{-1}. These vorticity estimates are used in a vorticity balance in Chapter V. Estimates of horizontal divergence also should be accurate within $\pm.22 \times 10^{-6}$ sec^{-1}. Indirect estimates of the order of magnitude of horizontal

Figure 3.1 Daily estimates of $\frac{\partial v}{\partial y}$ plotted against estimates of $\frac{\partial u}{\partial x}$ from MODE-0 Array 1 measurements. The correlation coefficient is calculated to be -0.93. The line is drawn to illustrate the condition of horizontal non-divergence. Typical errors are indicated.

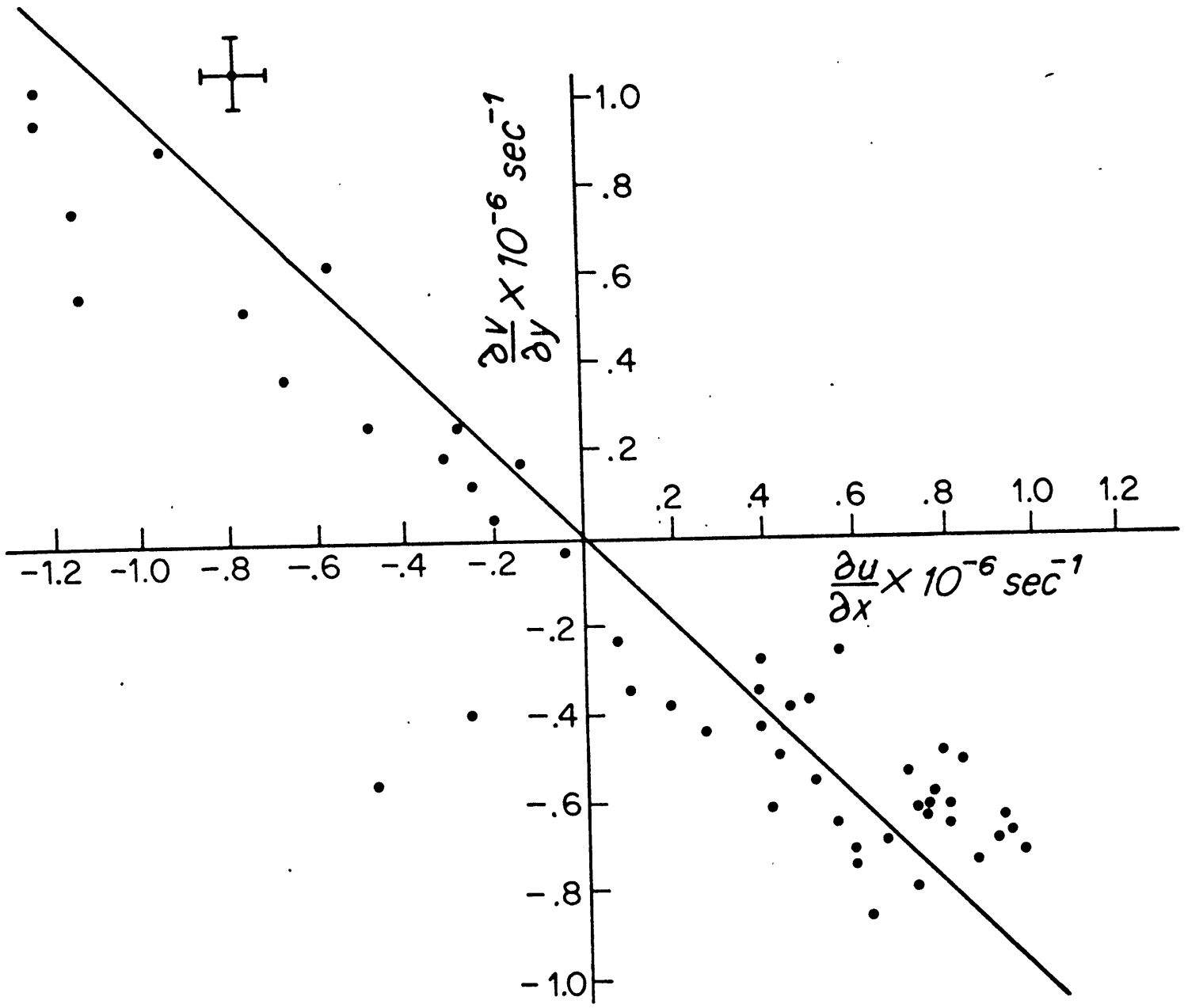
1.0
.8
.6
.4
.2
$\frac{\partial v}{\partial y} \times 10^{-6}\ sec^{-1}$
.2
.4
.6
.8
1.0
1.2
-1.2
-1.0
-.8
-.6
-.4
-.2
$\frac{\partial u}{\partial x} \times 10^{-6}\ sec^{-1}$
-.2
-.4
-.6
-.8
-1.0

Table 3.2

Tests for horizontal nondivergence from four-day averaged estimates of $\frac{\partial u}{\partial x}$ and $\frac{\partial v}{\partial y}$. Estimates of $\frac{\partial u}{\partial x}$ and $\frac{\partial v}{\partial y}$ have standard deviation errors of $\pm .15 \times 10^{-6}$ sec^{-1} due to measurement errors in velocity. Estimates of $\frac{\partial u}{\partial x}$ may be small by 2% and of $\frac{\partial v}{\partial y}$ small by 4% due to sampling errors. The tests are done for the ranges of $\frac{\partial u}{\partial x}$ and $\frac{\partial v}{\partial y}$ determined by these sampling errors. One asterisk (*) denotes a discrepancy from horizontal nondivergence of one to two standard deviations. Two asterisks (**) denote a discrepancy of two to three standard deviations.

Table 3.2

Time (Days)	$\frac{\partial u}{\partial x}$ 10^{-6} (sec^{-1})	$\frac{\partial v}{\partial y}$ 10^{-6} (sec^{-1})	$\frac{\partial u}{\partial x} + \frac{\partial v}{\partial y}$ 10^{-6} (sec^{-1})	Range in $\frac{\partial u}{\partial x}$ 10^{-6} (sec^{-1})	Range in $\frac{\partial v}{\partial y}$ 10^{-6} (sec^{-1})	
2	.69	-.69	.00	.69-.15 .70+.15	-.72-.15 -.69+.15	
6	.78	-.70	.08	.78-.15 .80+.15	-.73-.15 -.70+.15	
10	.86	-.63	.23	.86-.15 .88+.15	-.66-.15 -.63+.15	
14	.67	-.66	.01	.67-.15 .68+.15	-.69-.15 -.66+.15	
18	.87	-.61	.26	.87-.15 .89+.15	-.64-.15 -.61+.15	*
22	.46	-.50	-.04	.46-.15 .47+.15	-.52-.15 -.50+.15	
26	.41	-.36	.05	.41-.15 .42+.15	-.38-.15 -.36+.15	
30	-.11	-.42	-.53	-.11-.15 -.11+.15	-.44-.15 -.42+.15	**
34	-.46	.44	-.02	-.47-.15 -.46+.15	.44-.15 .46+.15	
38	-1.19	.83	-.36	-1.21-.15 -1.19+.15	.83-.15 .86+.15	*
42	-.55	.34	-.21	-.56-.15 -.55+.15	.34-.15 .35+.15	
46	-.13	.03	-.10	-.13-.15 -.13+.15	.03-.15 .03+.15	

Figure 3.2 Horizontal derivatives of velocity as a function of time during MODE-0. Estimated errors are $\pm .15 \times 10^{-6}$ sec^{-1} due to measurement errors in velocity and +4% in $\frac{\partial u}{\partial y}$, $\frac{\partial v}{\partial y}$ and +2% in $\frac{\partial u}{\partial x}$, $\frac{\partial v}{\partial x}$ due to sampling errors.

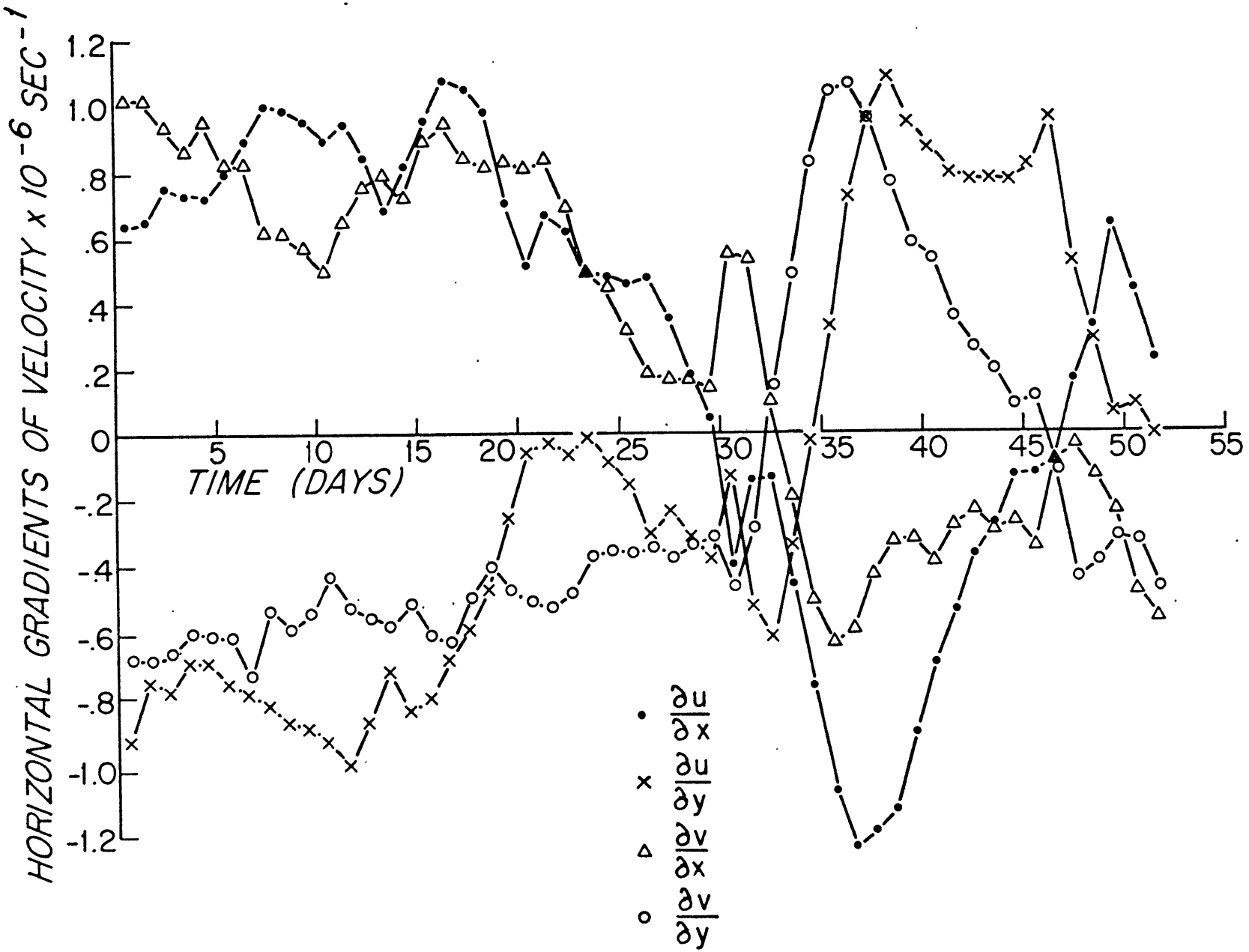
HORIZONTAL GRADIENTS OF VELOCITY x 10 -6 SEC -1
1.2
1.0
.8
.6
.4
.2
0
-.2
-.4
-.6
-.8
-1.0
-1.2
5
10
15
20
25
30
35
40
45
50
55
TIME (DAYS)
• ∂u/∂x
× ∂u/∂y
△ ∂v/∂x
○ ∂v/∂y

divergence from linear vorticity and heat balances, however, indicate that horizontal divergence should be of order 10^{-8} sec^{-1}, which is an order of magnitude smaller than the direct estimates (Table 3.3) and an order of magnitude smaller than the expected errors. Thus, the direct estimates of horizontal divergence are dominated by errors and are not accurate estimates of horizontal divergence.

To determine how small the errors in velocity measurements must be in order to make accurate estimates of horizontal divergence it is assumed that sampling and measurement errors should be equal and no larger than $1 \times 10^{-8} sec^{-1}$. For horizontal separations of 27 km the sampling error in estimates of horizontal derivatives of magnitude 7 cm/sec/60 km ($=1.2 \times 10^{-6}$ sec^{-1}) is 1×10^{-8} sec^{-1}. To obtain an error of 1×10^{-8} sec^{-1} for horizontal separations of 27 km, the error in velocity measurements must be reduced to .02 cm/sec which is substantially smaller than the error .45 cm/sec determined from IWEX measurements (Chapter I). The measurement error can be reduced by increasing the number of instruments. Five hundred current meters, however, would be needed to reduce the error to $\frac{.45}{\sqrt{500}} = .02$ cm/sec so that horizontal divergence could be estimated within 1×10^{-8} sec^{-1}. Unless the measurement error in velocity is reduced by an order of magnitude, it is unlikely that accurate estimates of horizontal divergence can be made directly from velocity measurements. Because the indirect estimates of horizontal divergence are presently an order of

Table 3.3

Comparison of direct and indirect estimates of horizontal divergence. Negative horizontal divergence, $\frac{\partial w}{\partial z}$, is calculated by three methods: 1) directly from estimates of $\frac{\partial u}{\partial x}$ and $\frac{\partial v}{\partial y}$; 2) indirectly from temperature measurements assuming a conservation of heat equation of the form $\frac{\partial T}{\partial t} + w\frac{\partial \overline{T}}{\partial z} = 0$ and a linear decrease of the vertical velocity from its value at 1500 m to zero at the bottom; and 3) indirectly from the linear vorticity equation according to $(\frac{\partial}{\partial t}\ (\frac{\partial v}{\partial x} - \frac{\partial u}{\partial y}) + \beta v)/f$.

Table 3.3

Time (Days)	$\frac{\partial w}{\partial z} = -(\frac{\partial u}{\partial x} + \frac{\partial v}{\partial y})$	$\frac{\partial w}{\partial z} = \frac{\partial T / \partial t}{\partial T / \partial z}_{3500m}$	$\frac{\partial w}{\partial z} = \frac{\frac{\partial}{\partial t}(\frac{\partial v}{\partial x} - \frac{\partial u}{\partial y}) + \beta v}{f}$
	($\times 10^{-8}$ sec^{-1})	($\times 10^{-8}$ sec^{-1})	($\times 10^{-8}$ sec^{-1})
5	8.6	-.33	-.72
10	11.6	2.15	.66
15	14.8	1.96	.80
20	10.5	-1.98	-1.48
25	-4.4	-.18	.32
30	-20.2	1.24	1.18
35	-32.9	-.68	-5.37
40	-24.8	-.03	-.03
45	-11.3	1.24	.20
Average Absolute Magnitude	15.5	1.09	1.18

magnitude smaller than the direct estimates, future attempts at estimating horizontal divergence should be made from a nonlinear heat balance or a nonlinear vorticity balance.

For measurements where the errors in velocity are not known a priori, I suggest that the divergence ratio, defined as

$$\frac{\Sigma\left|\frac{\partial u}{\partial x} + \frac{\partial v}{\partial y}\right|}{\Sigma\left|\frac{\partial u}{\partial x}\right| + \Sigma\left|\frac{\partial v}{\partial y}\right|}$$

where the summation is done over the number of time periods in the record length, be used to determine the errors in horizontal derivatives of velocity. This determination assumes that the horizontal divergence is nearly zero compared with the individual derivatives. A ratio near zero means that the measured velocity field is nearly horizontally nondivergent and hence has small errors. The ratio calculated for the measurements used here is about .14 for averaging periods of two days or longer (Table 3.4). Expressed as percentage error, the error of $.15 \times 10^{-6}$ sec^{-1} due to measurement errors becomes a 22% error in $\frac{\partial u}{\partial x}$ or $\frac{\partial v}{\partial y}$, so the divergence ratio is a realistic estimate of the errors in horizontal derivatives of velocity. This ratio calculated from MODE-1 velocity measurements is used in Chapter V in discussion of vorticity balance calculations. Several other ratios were considered and rejected. A ratio of net mass flux into or out of the array to the sum of ab-

Table 3.4

Averaging Period	$\frac{\Sigma\left\lvert\frac{\partial u}{\partial x}+\frac{\partial v}{\partial y}\right\rvert}{\Sigma\left\lvert\frac{\partial u}{\partial x}\right\rvert+\Sigma\left\lvert\frac{\partial v}{\partial y}\right\rvert}$
6 hours	0.47
12	0.33
18	0.26
24	0.20
30	0.22
36	0.19
42	0.20
48	0.16
54	0.16
60	0.16
66	0.18
72	0.15
1 day	0.18
2	0.14
3	0.14
4	0.14
5	0.13
6	0.13
7	0.14
8	0.13

Table 3.4. Divergence ratio calculated for various time averaging intervals. For periods of days velocities were first put through a low pass filter designed by Schmitz (1974).

solute mass fluxes across each side of the array was rejected because a large mean flow results in deceptively small estimated errors. A ratio of divergence to vorticity also was rejected because in some regions the velocity field may be nearly irrotational so that this ratio would result in deceptively large estimated errors.

Freeland (1975) and Swallow (private communication) have attempted tests of horizontal divergence with MODE-1 measurements. Freeland's comparisons in terms of transverse and longitudinal correlation functions are difficult to evaluate because of a lack of error analysis. From float measurements Swallow obtained values of horizontal divergence of order $.7 \times 10^{-6}$ sec^{-1} which is considerably larger than the errors obtained here of $\pm.22 \times 10^{-6}$ sec^{-1}.

Meteorologists recently have achieved apparent success in estimating horizontal divergence. From a 500 km square rawinsonde array Rasmusson (1971) claimed to estimate horizontal divergence accurately enough to calculate water vapor flux. The horizontal separations are so large, however, that sampling errors may be much larger than the estimates of horizontal divergence. Kung (1973) estimated horizontal divergence by as many as twenty-four different schemes and selected the estimate for which the vertical velocity became small above 250 mbar. The validity of these estimates is determined by their applicability in kinetic energy budgets (Kung, 1975). These budgets, however, have a dissipation term estimated as the residual of the calculated terms.

This residual is as large as the estimated terms so that errors in vertical velocity may be hidden in this residual dissipation. Thus, there are reasons to doubt the meteorologists' success in estimating horizontal divergence. Accurate estimation of horizontal divergence remains a problem for both meteorologists and oceanographers.

CONCLUSIONS

Velcoity measurements during MODE-0 Array 1 are horizontally nondivergent within estimated errors. The estimated error in values of horizontal divergence and vorticity is $\pm.22 \times 10^{-6}$ sec^{-1}. This error is as large as the standard deviation of estimates of horizontal divergence but only 19% as large as that of vorticity. Thus, vorticity but not horizontal divergence can be estimated accurately from these velocity measurements. This error is much larger than the expected magnitude of horizontal divergence based on indirect estimates of horizontal divergence. Measurement errors must be reduced by an order of magnitude before direct estimates of horizontal divergence can be made accurately. For this reason future estimates of horizontal divergence should be made from nonlinear heat or vorticity balances where estimates of horizontal divergence are smaller and have smaller errors than the direct estimates.

CHAPTER IV

HEAT BALANCE: HORIZONTAL ADVECTION OF TEMPERATURE

INTRODUCTION

By scale analysis horizontal advection should make an important contribution in causing local changes of heat for low-frequency currents. Wave theories, which provide most of the background for discussions of low-frequency current dynamics, assume only a minor role for horizontal advection in the heat balance and attribute local changes of temperature to vertical advection of the mean vertical temperature profile (Rhines, 1970). The success of the linear wave models in explaining the frequencies and spatial scales of observed current is often cited as a justification for the neglect of the nonlinear terms (Phillips, 1966; McWilliams and Robinson, 1974; McWilliams and Flierl, 1975). Because the nonlinear horizontal advection is necessary for energy transfer between scales and because nonlinear models may explain equally well the scales of observed currents, it is valuable to estimate the horizontal advection of temperature.

In this analysis of the heat balance from the IWEX measurements it is the vertical advection which is difficult to estimate since there are no measurements of vertical velocity. Estimates of local time changes and horizontal advection of temperature are compared to determine

the relative importance of horizontal advection. To the extent that horizontal advection balances local time changes of temperature the wave theories must be re-examined for their applicability in interpreting the measurements.

Calculations of local changes and horizontal advection of temperature are also important because it may be possible to infer values of vertical velocity from their sum. Because direct calculation of horizontal divergence was unsuccessful in the sense that the errors in w_z were larger than the estimates (Chapter III), an alternate estimate of vertical velocity is needed to calculate horizontal divergence in the vorticity balance (Chapter V). Provided the sum of local changes and horizontal advection of temperature is larger than its errors and larger than the divergence of the heat fluxes due to higher frequency motions, vertical velocity can be inferred from this sum.

The calculation of horizontal advection of temperature directly from estimates of horizontal gradients of temperature has large error. Estimates of temperature gradients used in geostrophic comparisons (Chapter II) had estimated errors between 1.4 and 2.6×10^{-8} °C/cm. These errors lead to errors in horizontal advection of temperature over four days for a current of 10 cm/sec of 0.072 to 0.133 °C, which are larger than the observed temperature changes during the measurements used here.

To avoid these large errors estimates of horizontal

advection of temperature are made by assuming a thermal wind balance (equation 2.8). Horizontal advection then can be estimated from the speed and turning about the vertical of the horizontal current (equation 4.4). Although this method of calculating horizontal advection of temperature was derived independently, some of the ideas were outlined and used previously (Miller and Thompson, 1942; Hide, 1971). This method is especially applicable to oceanic analysis since measurements on a single mooring are all that is needed to estimate horizontal advection of temperature. In addition, the errors for this calculation are smaller than expected errors in the calculation from estimates of horizontal gradients of temperature.

THEORY

The time averaged conservation of heat equation may be written:

$$\frac{\partial \overline{T}}{\partial t}+\overline{u}\frac{\partial \overline{T}}{\partial x}+\overline{v}\frac{\partial \overline{T}}{\partial y}+\overline{w}\left(\frac{\partial \overline{T}}{\partial z}+\rho g\Gamma\right) =$$

$$\kappa\left(\frac{\partial^2 \overline{T}}{\partial x^2}+\frac{\partial^2 \overline{T}}{\partial y^2}+\frac{\partial^2 \overline{T}}{\partial z^2}\right)-\frac{\partial}{\partial x}(\overline{u'T'})-\frac{\partial}{\partial y}(\overline{v'T'})-\frac{\partial}{\partial z}(\overline{w'T'}) \qquad (4.1)$$

where κ is the thermal diffusion coefficient, Γ is the adiabatic temperature gradient, bars ($\overline{\quad}$) represent time averages over a period of days and primes ($'$) represent deviations from time averages as in Chapter II. Fofonoff

(1962) has reviewed this equation and the time averaging procedure. The molecular diffusion terms are small for a large-scale problem. The eddy heat diffusion terms, $\frac{\partial}{\partial x}(\overline{u'T'}), \frac{\partial}{\partial y}(\overline{v'T'}), \frac{\partial}{\partial z}(\overline{w'T'})$, are considered small in a large-scale problem. This assumption is valid in this analysis of IWEX measurements only if the observed heat fluxes do not vary over length scales shorter than 10 km. Lastly, it is assumed that vertical advection of temperature can be represented by the vertical advection of the long-period mean vertical potential temperature gradient, $\overline{w}(\frac{\partial T}{\partial z}+\rho g\Gamma)=\overline{w}\frac{\partial \overline{\theta}_0}{\partial z}$, where the mean potential temperature, $\overline{\theta}_0(z)$, corresponds to $\overline{\rho}_0(z)$ defined in Chapter II (Veronis, 1973). The heat balance then becomes:

$$\frac{\partial \overline{T}}{\partial t}+\overline{u}\frac{\partial \overline{T}}{\partial x}+\overline{v}\frac{\partial \overline{T}}{\partial y}+\overline{w}\frac{\partial \overline{\theta}_0}{\partial z} = 0 \qquad (4.2)$$

$$(1) \quad (\frac{U}{\omega L}) \quad (\frac{N^2H^2}{\omega f L^2}\delta).$$

The non-dimensional numbers characterizing the size of each term are written in parentheses below each term. In order to estimate the scale magnitude of $w\frac{\partial \theta_0}{\partial z}$ the thermal wind relations (equations 2.8) are assumed and because of the geostrophic balance and the continuity equation (equation 3.3) the magnitude of $\overline{w}$ is taken to be $\delta \frac{H}{L} U$ where δ is defined after equation 3.3. N is the Brunt-Väisälä frequency, $\sqrt{\frac{g}{\rho}(\frac{\partial \rho}{\partial T}\frac{\partial \overline{\theta}_0}{\partial z} + \frac{\partial \rho}{\partial S}\frac{\partial \overline{S}_0}{\partial z})}$, where S is salinity.

For $U = 10$ cm/sec, $L = 60$ km, $\omega = 1/10$ days, $H = 1$ km (Gould, Schmitz and Wunsch, 1974) and $N = 2.5$ cph (Millard and Bryden, 1973), these non-dimensional numbers are of order 1: $\frac{U}{\omega L} = 1.4$ and $\delta\frac{N^2H^2}{\omega f L^2} = 1.6$. Thus, no simple two term balance is evident for the heat conservation equation.

Use of the thermal wind equations (2.8) allows a simplification to be made in the advective terms of the conservation equation:

$$u\frac{\partial T}{\partial x} + v\frac{\partial T}{\partial y} = \frac{\rho_0 f}{g\alpha}\left(u\frac{\partial v}{\partial z}\,(1\pm 0(\varepsilon)) - v\frac{\partial u}{\partial z}\,(1\pm 0(\varepsilon))\right) \qquad (4.3)$$

where ε is the largest of $(\frac{\omega}{f}, \frac{U}{fL}, \frac{U'}{fL'}, \frac{\nu}{fH^2}, \frac{\nu}{fL^2}, \frac{H}{L})$. A transformation to notation with horizontal velocity described by speed, S, and direction measured counterclockwise from East, θ, leads to further simplification:

$$u\frac{\partial T}{\partial x} + v\frac{\partial T}{\partial y} = \frac{\rho_0 f}{g\alpha}\left[S^2\,\frac{\partial\theta}{\partial z}\,(1\pm 0(\varepsilon)) \pm 0(\varepsilon)\,\frac{\partial}{\partial z}\,(S^2/2)\right]. \qquad (4.4)$$

Thus, the advection of heat may be represented as a function only of the speed and the turning about the vertical of the horizontal current.

Only low-frequency motions which are nearly geostrophic and hydrostatic in an ocean with a tight T/S relationship satisfy this representation. The theoretical errors due to assumption of geostrophic and hydrostatic balances can be estimated from the measurements needed for the calculation. The more nearly geostrophic and hydrostatic the motions are,

the smaller these theoretical errors are. Theoretical errors due to the scatter in the T/S relationship are discussed in the next section.

DATA AND METHODS

Estimates of local time changes of temperature and of horizontal advection of temperature are calculated from measurements of current and temperature on the IWEX mooring. The IWEX mooring, in the shape of a tetrahedron, had three instruments measuring current and temperature at each of six depths: 606, 611, 640, 731, 1023, 2050 m (Briscoe, 1975). The instruments were separated horizontally by 6.1 m at 606 m depth and by 1600 m at 2050 m depth. Four-day averaged currents and temperature changes are assumed to be the same for measurements at the same depth so that average current and temperature change are obtained at each depth for each four-day period. The direction of horizontal current changed monotonically between 731 m and 2050 m so this depth interval is used in the calculations. For shallower depths direction did not change monotonically.

Vertical averages of local time change of temperature over four days, $\Delta T_{average}$, are calculated by application of the trapezoidal rule:

$$\Delta T_{average} = 0.5\ \Delta T_{1023m} + 0.11\ \Delta T_{731m} + 0.39\ \Delta T_{2050m}. \qquad (4.5)$$

The error in individual temperature changes has standard deviation .003°C (Chapter I) but the error in $\Delta T_{average}$ is only .002°C due to the repeated measurements. The estimate $\Delta T_{average}$ is 26% larger than the value obtained from a first baroclinic mode between 731 and 2050 m depths.

Vertical averages of horizontal advection of temperature over four days are estimated according to the formula:

$$u \cdot \nabla T = \frac{1}{\Delta H} \frac{\rho_0 f}{g} \int_{t_0}^{t_0 + 4\text{days}} dt \int_{-2050\text{m}}^{-731\text{m}} dz \, \frac{S^2}{\alpha} \frac{\partial \theta}{\partial z} =$$

$$\frac{\rho_0 f}{g\alpha} S^2_{1023} \quad \frac{\theta_{731} - \theta_{2050}}{1319 \text{ m}} \times 4 \text{ days} \qquad (4.6)$$

The error in this estimate for S = 10 cm/sec is .008°C due to measurement errors in direction and 5% due to measurement errors in speed. It is estimated that errors in α are 5%. To obtain estimates of sampling errors this estimate is compared with the vertical average obtained from a combination of first baroclinic mode of amplitude 10 cm/sec at 700 m depth and a barotropic velocity of amplitude 2 cm/sec perpendicular to the baroclinic velocity. This estimate is 19% larger than the value from the combination. Due to sampling errors in time integration this estimate is 1% smaller than the value obtained from continuous integration for a frequency 1/10 days.

There are additional errors in the estimates of horizontal advection due to assumption of a thermal wind bal-

ance. For $U = 10$ cm/sec, $L = 60$ km $\varepsilon = .025$ the theoretical errors are of size $.025\frac{\rho_0 f}{g\alpha}(S^2\frac{\partial\Theta}{\partial z}\pm\frac{\partial}{\partial z}S^2/_2)\times$ 4 days according to equation 4.4. For the measurements considered here these errors are less than .003°C. Larger errors in the estimates of horizontal advection arise from the scatter in the T/S correlation. Thermal wind equations in the ocean are in terms of horizontal gradients of density (equation 2.7). It is the tightness of the T/S relationship that allows the thermal wind equations to be written in terms of temperature. From carefully calibrated CTD stations over a 10 km square area (Millard, private communication) it is estimated that temperature can vary by ±.04°C without a change in density. This variation may be due to a limitation in ability to measure salinity in which case the variation is not an error in estimates of horizontal advection of temperature. A change in salinity of .005 $^{o}/_{oo}$ between CTD stations could account for the entire scatter in the T/S relationship. At present, the scatter does exist so an error of 0.04°C must be included in estimates of horizontal advection of temperature.

RESULTS AND DISCUSSION

Estimates of local time changes of temperature are of opposite sign from and of approximately the same magnitude as estimates of horizontal advection of temperature (Figure 4.1). The correlation coefficient between daily estimates of local change and horizontal advection (Figure

Figure 4.1. Four-day averaged estimates of local time change of temperature (- - - -) and negative horizontal advection of temperature (———) from IWEX measurements. Estimates of horizontal advection are made by assuming a thermal wind balance. Time changes and horizontal advection are averages over the depth interval 731 to 2050m according to equations 4.4 and 4.5. Negative horizontal advection is plotted to facilitate visual comparison.

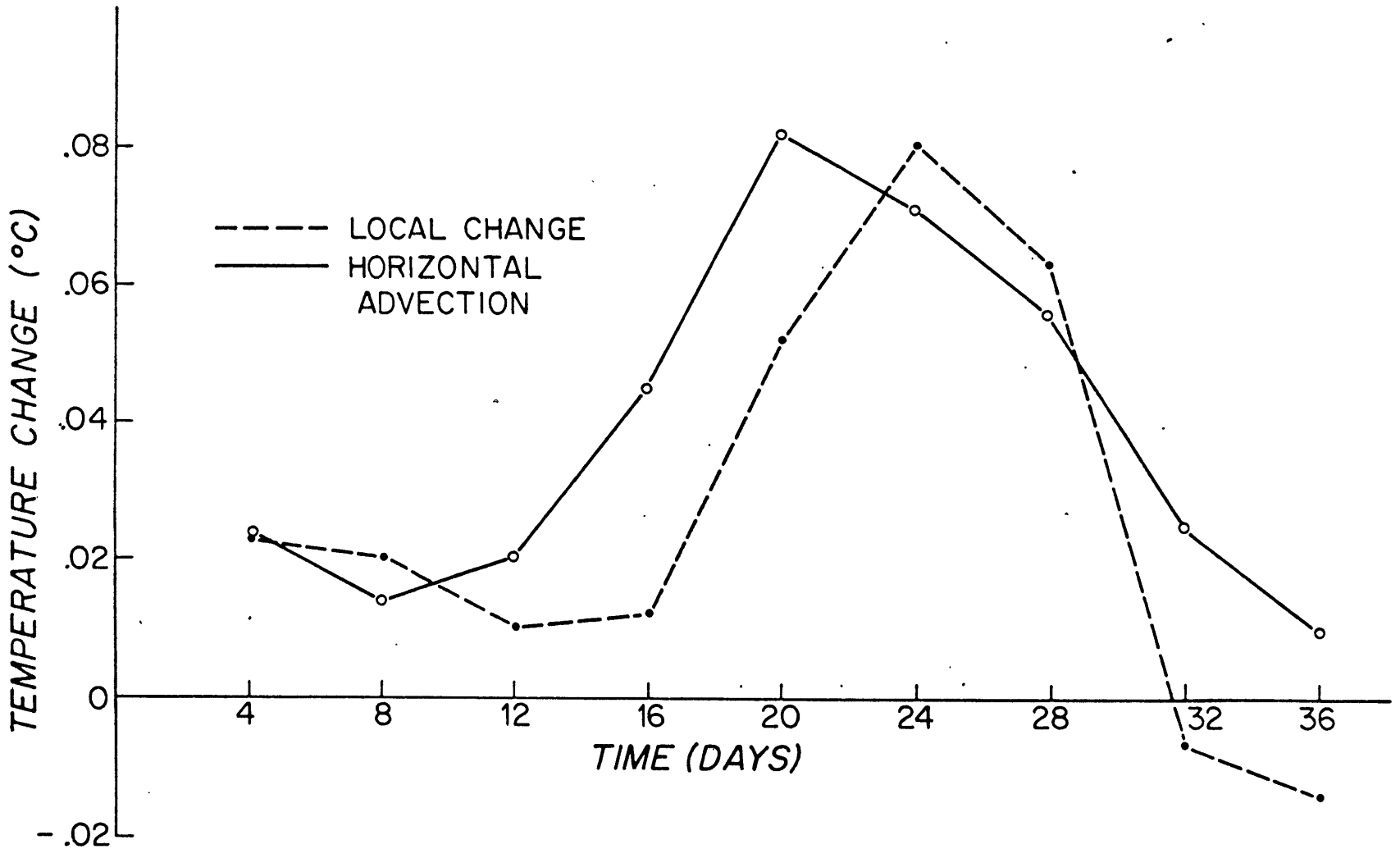
LOCAL CHANGE
HORIZONTAL ADVECTION
TEMPERATURE CHANGE (°C)
.08
.06
.04
.02
0
-.02
4
8
12
16
20
24
28
32
36
TIME (DAYS)

4.2) is -0.65 which is significantly nonzero at a 95% confidence level. Horizontal advection accounts for 73% of the variance in the local changes of temperature. Within estimated errors there is a balance between local changes and horizontal advection of temperature (Table 4.1).

Because most of the error in estimates of horizontal advection is due to observed scatter in the T/S relationship which may be due to measurement errors in salinity and hence not an error in these estimates of horizontal advection, a comparison is made of local changes with horizontal advection without the 0.04°C error due to T/S scatter (Figure 4.3). Because the sum of local changes and horizontal advection is larger in most cases than the remaining errors, the sum may represent vertical advection so that values of vertical velocity could be estimated.

To be sure that the sum represents vertical advection it is necessary to show that the divergence of the heat fluxes due to higher frequency motions are small. Heat fluxes calculated for the IWEX measurements show such small variations over horizontal separations of up to 2 km that they are probably due to instrument noise. If the heat fluxes vary only over eddy-scale distances as in the work of Müller and Olbers (Müller, 1975) their divergence is indeed small. Thus, it is plausible that for future measurements, where larger temperature changes are observed (Riser, 1975) or where local changes are not balanced by horizontal advection, estimates of vertical advection from

Figure 4.2. Daily estimates of local time change (----) and negative horizontal advection (——) of temperature. Estimates are made as described in figure 4.1.

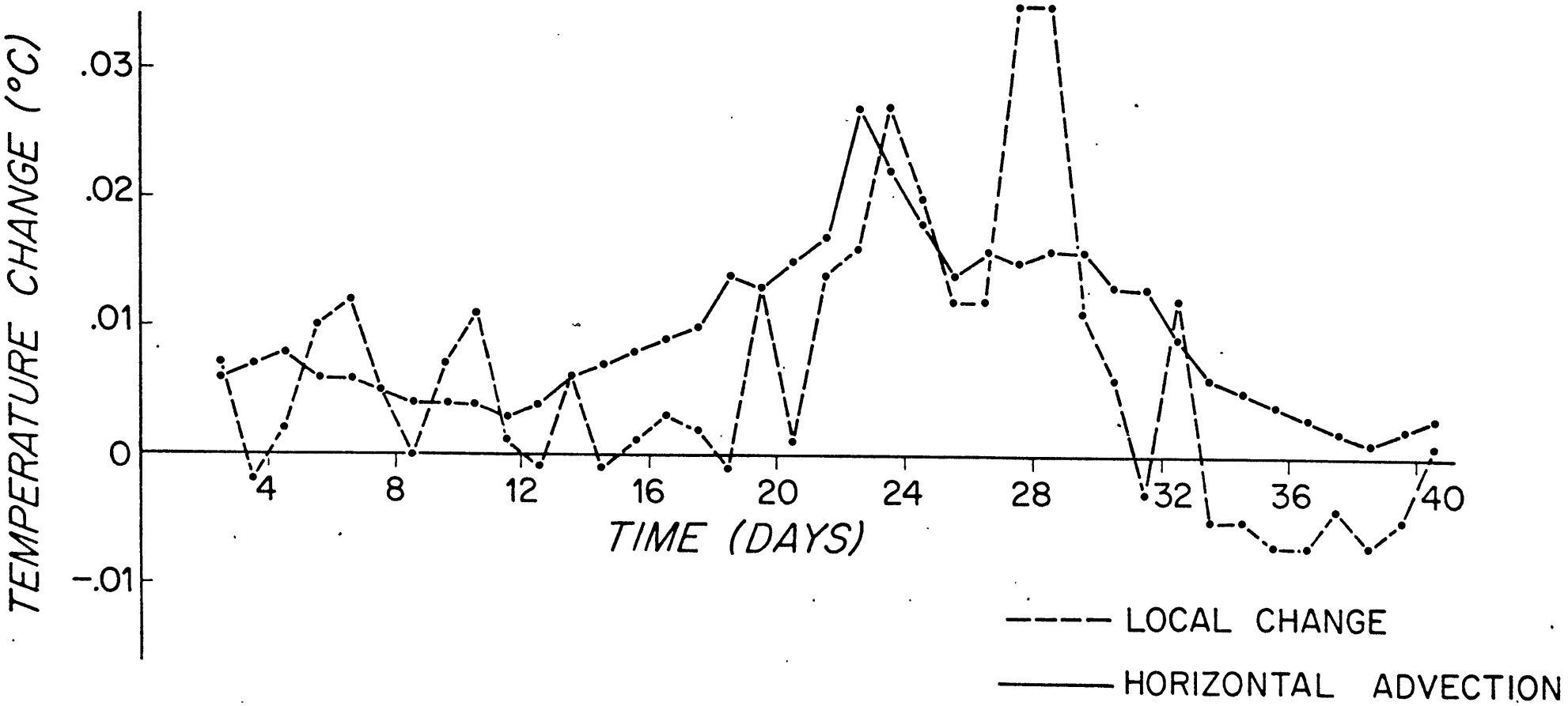
TEMPERATURE CHANGE (°C)
.03
.02
.01
0
-.01
4
8
12
16
20
24
28
32
36
40
TIME (DAYS)
LOCAL CHANGE
HORIZONTAL ADVECTION

Table 4.1

Comparison of local time change and horizontal advection of temperature over four day periods. Estimates of local change are made from $\int dt \frac{\partial T}{\partial t} = T_{n+1} - T_n$ where T_{n+1}, T_n are successive four-day averages; estimates of horizontal advection are made from $u \cdot \nabla T \, dt = \frac{\rho_0 f}{g\alpha} S^2_{1023} \frac{\theta_{731} - \theta_{2050}}{1319 \text{ m}} \times$ 4 days where S, θ are the speed and direction of four-day averaged velocity. Error ranges are determined by taking into account measurement, sampling, and theoretical errors. Within these errors there is a balance between local change and horizontal advection of temperature.

Table 4.1

Time (Days)	Local Change of Temperature (deg C)	Horizontal Advection of Temperature (deg C)	Local Change + Horizontal Advection (deg C)	Range in Local Change of Temperature (deg C)	Range in Horizontal Advection of Temperature (deg C)
4	.023	-.024	-.001	.018 ± .002	-.020 ± .041
8	.020	-.014	+.006	.016 ± .002	-.012 ± .041
12	.010	-.020	-.010	.008 ± .002	-.017 ± .041
16	.012	-.045	-.033	.009 ± .002	-.038 ± .041
20	.052	-.082	-.030	.041 ± .002	-.069 ± .042
24	.080	-.071	+.009	.063 ± .002	-.060 ± .041
28	.063	-.056	+.007	.050 ± .002	-.047 ± .041
32	-.007	-.025	-.032	-.006 ± .002	-.021 ± .041
36	-.014	-.010	-.024	-.011 ± .002	-.010 ± .040

Figure 4.3 Four-day averaged estimates of local time change (----) and negative horizontal advection of temperature with error estimates. Estimates are made as described in figure 4.1 . Error bars represent uncertainties due to measurement errors in speed, direction, and temperature and theoretical errors due to deviation from geostrophic and hydrostatic balances and to errors in estimates of $\alpha = -\frac{d\rho}{dT}$. Estimates are scaled to smaller values to take account of sampling errors due to finite difference calculations on a curved first baroclinic mode profile. Theoretical errors due to scatter in the T/S relationship are not included.

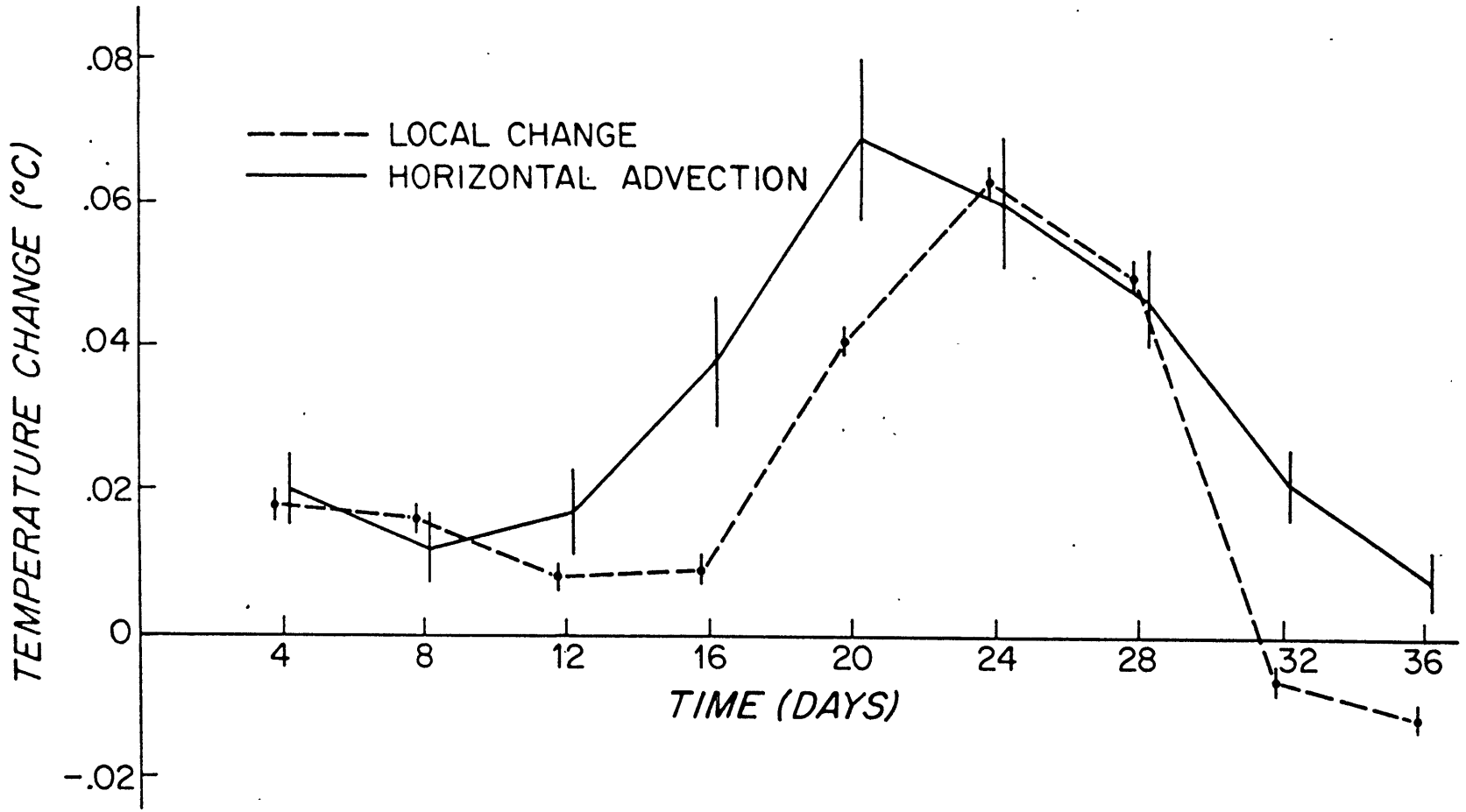
LOCAL CHANGE
HORIZONTAL ADVECTION
TEMPERATURE CHANGE (°C)
.08
.06
.04
.02
0
-.02
4
8
12
16
20
24
28
32
36
TIME (DAYS)

the sum of local change plus horizontal advection can be used to estimate vertical velocities.

The result that horizontal advection of temperature is comparable in magnitude with the local time change of temperature and in fact balances local change casts doubt on the applicability of linear theories which assume local changes of temperature are due to vertical advection and horizontal advection is unimportant (Rhines, 1970). Local fits of observations by a number of linear waves (Phillips, 1966; McWilliams and Robinson, 1974; McWilliams and Flierl, 1975) are also suspect since their assumption that local changes of temperature are due to vertical advection is violated. Phillips (1966) noted that the assumption of linearity was tenuous but argued that the low mean velocities in regions away from the Gulf Stream should rule out the importance of mean flow advection. McWilliams and Robinson (1974) and McWilliams and Flierl (1975) examine the importance of nonlinearity after doing the wave fits by calculating the wave-wave interactions. For POLYGON (Koshlyakov and Grachev; 1973) and MODE-0 Array 1 wave fits these interactions were small while for MODE-1 they are large. Despite the large wave-wave interactions McWilliams and Flierl remain optimistic that the goodness of the MODE-1 wave fit indicates the validity of the linear solutions. The results presented here, although they are for the IWEX measurements which were in the MODE region but

during a later period, conflict with this optimism by showing that advection is as important as local time changes in the local dynamics and that the vertical velocity is smaller than linear theory predicts. These results also suggest that the time scale of change following a fluid parcel may be much longer than the time scale of local change.

The numerical experiments of Rhines (1975) and Holland and Lin (1975) help explain this conflict between the success of linear wave models and the importance of horizontal advection. In experiments on barotropic currents Rhines found that even though the linear and nonlinear terms were of the same size something similar to the westward phase propagation of linear waves occurred. In their experiments on ocean circulation Holland and Lin also found that advection was important in the local dynamics while eddies moved westward at approximately Rossby-wave velocities. On the basis of these experiments the wave fits can describe qualitatively the scales and propagation velocities of oceanic eddies despite the fact that horizontal advection is important in the local dynamics.

Linear models, while they may describe eddy scales and movement, are inadequate to investigate the formation and decay of eddies since the linear solution allows no energy

transfer between scales and allows energy flux only through group velocity. While westward phase propagation was occurring in Rhines's (1975) experiments, energy was being transferred into longer spatial scales. In Holland and Lin's (1975) experiments the eddies grew by conversion of the mean potential energy and the mean currents were driven by the Reynolds stresses associated with the eddies. These transfers of energy were possible because of the presence of significant nonlinearity in the models. Nonlinear dynamics are required to allow energy exchange between various scales.

The importance of horizontal advection during the IWEX measurements suggests that energy transfer should be examined. Because the time period (40 days) and horizontal spacing (< 2 km) of the measurements are not large enough to determine the scales involved in the energy transfer, it is necessary to investigate the question of energy transfer during the IWEX measurements in terms of a specific model. The specific model used here is that of baroclinic instability which predicts growth of perturbation waves by conversion of potential energy contained in the mean flow (Eady, 1949). Although this model is appropriate for infinitessimal waves, attempts often are made to apply it to observations of finite-amplitude features (Green, 1970).

The baroclinic instability model requires the assumption of a mean velocity and a vertical shear of mean velocity to linearize the theoretical problem. The energy transfer is then between the mean flow and perturbation

wave only. For this model the heat balance is written:

$$\frac{\partial T'}{\partial t} + \bar{U}\frac{\partial T'}{\partial x} + v'\frac{\overline{\partial T}}{\partial y} + w'\frac{\overline{\partial T}}{\partial z} = 0$$

where T', v', w' are perturbation wave quantities; $\bar{U}$, $\frac{\overline{\partial T}}{\partial z}$ and $\frac{\overline{\partial T}}{\partial y} = \frac{-\rho_0 f}{g\alpha}\frac{\partial \bar{U}}{\partial z}$ are mean flow quantities. The long-time averaged mean velocity at 1400 m depth, the approximate mean depth of these IWEX measurements, is less than 1 cm/sec (Freeland, Rhines and Rossby, 1975) and the vertical shear of the mean current is less than .5 cm/sec/1000 m (McWilliams, 1974). For the velocities and shears observed during IWEX the advection by the long-time averaged mean flow field is not sufficient to account for the observed magnitude of the horizontal advection of temperature (Figure 4.1). A mean flow of 4 cm/sec and shear of 2 cm/sec/1000 m are needed to explain the observed advection in terms of mean flow advection. This result is similar to that obtained by Freeland, Rhines and Rossby (1975) who noted that mean flow advection could not account for their observed westward pattern propagation velocity of 5 cm/sec. They went on to conclude that the westward pattern movement must be due to wave propagation whereas for the IWEX measurements horizontal advection must be important. The conclusion then is that the long-time averaged mean flow field is not a significant contributor to the observed horizontal advection during IWEX.

During the forty-day IWEX period there was an average velocity of 4 cm/sec and average shear of 3 cm/sec/1000 m at 1400 m depth. The magnitude of the observed horizontal advection of temperature can be explained in terms of advection by this forty-day averaged flow field. This illustrates how carefully the mean flow must be defined when linearizing the equations about a mean state. The forty-day averaged flow field must be slowly changing over longer time periods in order to result in a long-time averaged velocity of less than 1 cm/sec. The following results in terms of a baroclinic instability model concern the growth of a perturbation wave by conversion of potential energy from the forty-day averaged flow field. It should be noted that this use of baroclinic instability is not standard since the long-time averaged flow field, generally used in baroclinic instability models (Gill, Green and Simmons, 1974) is smaller than the observed forty-day averaged flow field. Because the model equations used here differ from standard baroclinic instability equations only in the definition of the mean field, the term baroclinic instability is maintained.

In the baroclinic instability model, the horizontal advection of temperature should be of opposite sign from the local time change of temperature and from the vertical advection of the mean vertical temperature gradient (Bryan, 1974). For maximum release of mean potential energy the particle path of the perturbation parallel to (v', w') is at

an angle from the horizontal equal to one-half the angle of isentropic surfaces from horizontal (Green, 1960). For this maximum release, the magnitude of the horizontal advection of temperature should be twice as large as the local time change or the vertical advection. For the estimates from IWEX measurements (Table 4.1):

$$\frac{\partial T}{\partial t} = -.8(u\cdot\nabla T) \text{ and } w\frac{\partial T}{\partial z} = -(\frac{\partial T}{\partial t}+u\cdot\nabla T) = -.45(u\cdot\nabla T)$$

so the magnitudes and signs of the estimates are consistent with the instability model.

Because the baroclinic instability model assumes a perturbation wave periodic in space, there must be a phase lag in time between the local time change of temperature and horizontal advection of temperature in order for conversion of energy to occur. The purpose of the vertical phase function in the perturbation stream function used by Gill, Green and Simmons (1974) is to create a phase lag in time at each depth such that horizontal advection leads local change of temperature. To test for this phase difference in the IWEX measurements, cross-correlations as a function of time lag between daily estimates of horizontal advection and local time change of temperature (Figure 4.2) are calculated. Minimum (because the correlations are negative) correlation, -.71, occurs when horizontal advection leads local change by one day. This minimum correlation is not significantly less than the correlation for no time lag,

-.65, at a 95% confidence level which implies that the energy conversion is not statistically different from zero. The sign of the observed phase lag, however, is consistent with the baroclinic instability model.

The growth rate of the perturbation wave amplitude can be estimated from the phase lag by which horizontal advection leads local change of temperature, Δt, and the frequency of the wave, ω. The doubling time is of order $(\omega^2 \Delta t)^{-1}$ which is 100 days for Δt = 1 day and ω = 1/10 days (This frequency is taken from Gould, Schmitz and Wunsch's (1974) analysis of measurements at 1500 m depth in this region.). Such a doubling time is similar to estimates made by Robinson and McWilliams (1974) on theoretical grounds. Finer resolution of the phase lag and perturbation wave frequency would enable more accurate estimates of growth rates to be made.

For the IWEX measurements the estimates of local change, horizontal advection, and vertical advection of temperature and the estimated phase lag between horizontal advection and local change are consistent with the growth of a perturbation wave by conversion of potential energy contained in the forty-day averaged flow field. Longer time series of measurements on a single mooring are needed to establish the significance of a one-day lag between horizontal advection and local change. To investigate the transfer of energy I suggest that, because of the availability of oceanic time series of temperature and current,

moored measurements should be used to search for this phase lag in time rather than carry out the intense hydrographic survey suggested by Bryan (1974) to search for the vertical phase function of Gill, Green and Simmons (1974).

CONCLUSIONS

For IWEX measurements between 731 and 2050 m depths the local time change of temperature is balanced by horizontal advection of temperature within estimated errors. This balance could be established only because a representation of horizontal advection as a function of the speed and turning about the vertical of the horizontal current has small errors.

This balance between local change and horizontal advection rules out the applicability of strictly linear theoretical models. Quasi-linear models may still be relevant. Linearization about a mean flow field defined by the forty-day averaged currents can explain the observed magnitude of the horizontal advection of temperature. Comparisons with the quasi-linear baroclinic instability model indicate that the estimates of local change and horizontal advection of temperature are consistent with the growth of a perturbation wave by the conversion of potential energy in the forty-day averaged flow field. In particular, a phase lag in time is observed such that horizontal advection leads local change, though the lag is not statistically different from zero, as predicted by the instability model.

CHAPTER V

VORTICITY BALANCE

INTRODUCTION

Because the horizontal momentum equations are so dominated by the geostrophic balance, it is necessary to work with the higher-order vorticity balance to understand the evolution of time-varying ocean currents. In the vorticity balance the relative importance of horizontal advection of relative vorticity, $u\frac{\partial \zeta}{\partial x} + v\frac{\partial \zeta}{\partial y}$, of advection of planetary vorticity, βv, and of vortex stretching, $f\frac{\partial w}{\partial z}$, in causing local time change of vorticity, $\frac{\partial \zeta}{\partial t}$, is not known for ocean currents. By scaling arguments all are of the same magnitude. Estimates of these terms from measurements then are valuable for an understanding of the current dynamics. Because most models of ocean currents are based on specific balances of terms in the vorticity equation, these estimates also can be used to differentiate among various models.

Unfortunately, there are no measurements suitable for estimating either the horizontal advection or vortex stretching in a vorticity balance. Here, MODE-0 Array 1 measurements are used to test for balance between local change and planetary advection, and some reasonable, but inaccurate, estimates of vortex stretching are made. Also, an analysis is made for the expected errors in estimates of each of the terms in the vorticity balance (equation 5.1) and an ex-

periment is suggested in which all terms can be estimated with errors smaller than the expected magnitudes of the terms.

THEORY

The equation for the conservation of vorticity, $\bar{\zeta} = \frac{\partial \bar{v}}{\partial x} - \frac{\partial \bar{u}}{\partial y}$, is obtained by eliminating pressure from the horizontal momentum balances (equations 2.2):

$$\frac{\partial \bar{\zeta}}{\partial t} + \bar{u}\frac{\partial \bar{\zeta}}{\partial x} + \bar{v}\frac{\partial \bar{\zeta}}{\partial y} + \beta \bar{v} = f\frac{\partial \bar{w}}{\partial z} \qquad (5.1)$$

$$(1) \qquad \left(\frac{U}{\omega L}\right) \qquad \left(\frac{\beta L}{\omega}\right) \quad \left(\varepsilon \frac{f}{\omega}\right)$$

where β is the northward derivative of the Coriolis parameter, ε is defined after equation 2.7, the viscous terms and Reynolds stresses are neglected, and nonlinear terms involving vertical velocity are small because of the predominant geostrophic balance. Charney (1973) has discussed the derivation of this equation in detail. The nondimensional number characterizing the size of each term is written in parentheses below each term. For $U = 10$ cm/sec, $L = 60$ km, $\omega = 1/10$ days and $\beta = 2.0 \times 10^{-13}$ cm^{-1} sec^{-1}, $\frac{U}{\omega L} = 1.4$ $\frac{\beta L}{\omega} = 1.0$ and $\varepsilon \frac{f}{\omega} = 1.4$ so on scaling arguments all terms are of the same size.

In estimating horizontal advection of relative vorticity it is useful to use horizontal nondivergence as in equations 2.10 to obtain:

$$\bar{u}\frac{\partial\bar{\zeta}}{\partial x}+\bar{v}\frac{\partial\bar{\zeta}}{\partial y} = \frac{\partial}{\partial x}(S^2\frac{\partial\theta}{\partial x})+\frac{\partial}{\partial y}(S^2\frac{\partial\theta}{\partial y}) \pm 0(\delta)\sqrt{2}\frac{(u\frac{\partial u}{\partial x}\pm v\frac{\partial v}{\partial y})}{\Delta x} \qquad (5.2)$$

where Δx is the horizontal separation of the measurements and δ is defined after equation 3.3. For $U = 10$ cm/sec, $L = 60$ km, $\omega = 1/10$ days and horizontal separations of 50 km, this theoretical error, $\frac{\delta\sqrt{2}(u\frac{\partial u}{\partial x}\pm v\frac{\partial v}{\partial y})}{\Delta x}$, is $.11 \times 10^{-12}$ sec^{-2}.

DATA AND METHODS

From MODE-0 Array 1 measurements (Figure 1.1 and Table 3.1) estimates of local time change of vorticity, $\frac{\partial\zeta}{\partial t}$, and advection of planetary vorticity, βv, are made. The procedure for estimating vorticity is described in Chapter III. Estimates of vorticity (Figure 5.1) have errors of $\pm.22 \times 10^{-6}$ sec^{-1} and may be small by $2\%\frac{\partial v}{\partial x} - 4\%\frac{\partial u}{\partial y}$ due to sampling errors. Time changes of vorticity (Table 5.1) are obtained from differences of five-day averaged values of vorticity. These estimates have errors of $\pm.71 \times 10^{-12}$sec^{-2} due to measurement errors and may be small by 1% due to temporal sampling errors. The spatial sampling errors are less than $.32 \times 10^{-12}$ sec^{-2}. Estimates of planetary advection (Table 5.1) are made by averaging five-day averaged northward velocities for the four current meters and multiplying by $\beta = 2.0 \times 10^{-13}$ cm^{-1} sec^{-1}. These estimates have errors of $\pm.45 \times 10^{-13}$ sec^{-2} due to measurement errors and may be small by 9% due to spatial sampling errors. A correlation

Figure 5.1 Daily estimates of relative vorticity, $\frac{\partial v}{\partial x} - \frac{\partial u}{\partial y}$, from MODE-0 Array 1 measurements of velocity at 1500 m depth.

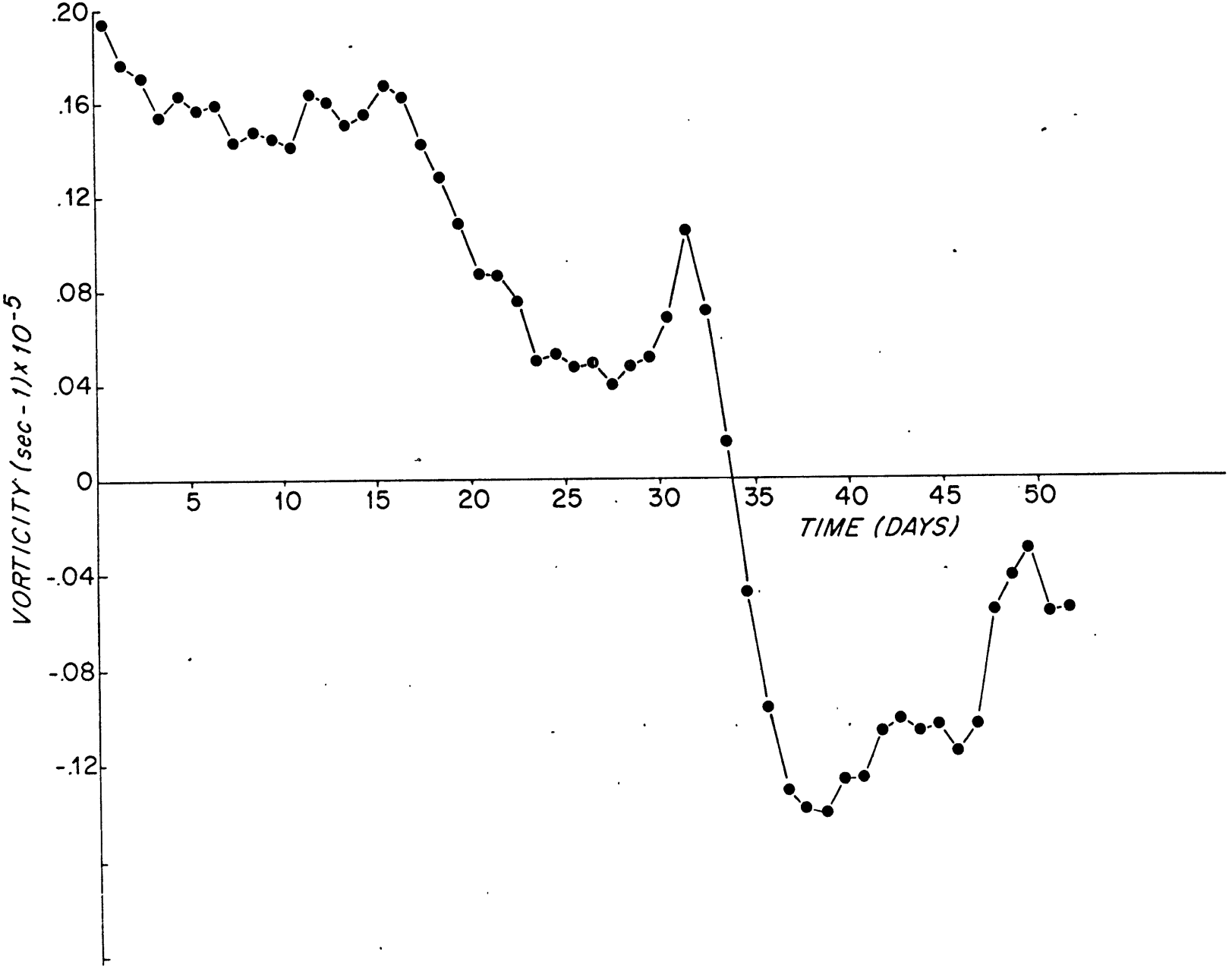
.20
.16
.12
.08
.04
0
-.04
-.08
-.12
VORTICITY (sec - 1) x 10-5
5
10
15
20
25
30
35
40
45
50
TIME (DAYS)

Table 5.1

Time	$\frac{\partial}{\partial t}(\frac{\partial v}{\partial x} - \frac{\partial u}{\partial y})$	βv
(Days)	($\times 10^{-12}$ sec^{-2})	($\times 10^{-12}$ sec^{-2}
5	-.48	-.01
10	.02	.43
15	-.24	.79
20	-1.87	.86
25	-.53	.75
30	.19	.62
35	-3.93	.26
40	.16	-.18
45	.70	-.56

Table 5.1. Comparison of local time change of vorticity with advection of planetary vorticity for MODE-0 Array 1 measurements. The time change of vorticity, $\frac{\partial}{\partial t}(\frac{\partial v}{\partial x} - \frac{\partial u}{\partial y})$, is estimated by differencing five-day averaged values of vorticity and dividing by five days. The advection of planetary vorticity is estimated by averaging five-day averaged northward velocities over the four current meters and multiplying by the northward derivative of the Coriolis parameter $\beta = 2.0 \times 10^{-13}$.

coefficient for these estimates of local change and planetary advection is calculated and tested against a null hypothesis of zero correlation.

Estimates of vortex stretching (Table 5.2) are made by assuming a linear heat balance, $w = -\frac{\partial T}{\partial t}/\frac{\partial \overline{T}}{\partial z}$ and a linear decrease in vertical velocity from its value at 1500 m to zero at the ocean bottom. As discussed in Chapter III these estimates are reasonable but because of the neglect of horizontal advection of temperature, shown to be important in Chapter IV, and because of the large sampling errors they have errors at least as large as the estimates. A correlation coefficient between these estimates of vortex stretching and the estimates of local change of vorticity plus planetary advection (Table 5.2) is calculated and tested for significance.

To reduce the errors in these estimates, time-integrated balances are calculated. The change in vorticity over the measurement period, $\zeta_{end} - \zeta_{start}$, is compared with the change in planetary vorticity due to net northward flow, $\beta \int_{start}^{end} dt\ v$.

The error in the change of vorticity is $\pm .31 \times 10^{-6}$ sec^{-1} due to measurement errors and $2\%(\frac{\partial v}{\partial x}$ end $-\frac{\partial v}{\partial x}$ start) + $4\%(\frac{\partial u}{\partial y}$ start $-\frac{\partial u}{\partial y}$ end) $= -.07 \times 10^{-6}$ sec^{-1} due to sampling errors. The error in the change of planetary vorticity is $\pm .06 \times 10^{-6}$ sec^{-1} due to measurement errors and $+9\% = +.12 \times 10^{-6}$ sec^{-1} due to sampling errors. The sum of

Table 5.2

Time	$\frac{\partial}{\partial t}(\frac{\partial v}{\partial x} - \frac{\partial u}{\partial y}) + \beta v$	$f \frac{\partial w}{\partial z}$
(Days)	($\times 10^{-12}$ sec^{-2})	($\times 10^{-12}$ sec^{-2})
5	-.49	-.22
10	.45	1.47
15	.55	1.34
20	-1.01	-1.36
25	.22	-.12
30	.81	.85
35	-3.67	-.47
40	-.02	-.02
45	.14	.85

Table 5.2. Comparison of the sum of local time change of vorticity plus advection of planetary vorticity with vortex stretching for MODE-0 Array 1 measurements. Estimates of the time change of vorticity and the planetary advection are obtained from Table 5.1. The horizontal divergence is obtained from temperature measurements on two moorings by assuming a linear heat balance so that $w = -\frac{\partial T}{\partial t} / \frac{\partial \overline{T}}{\partial z}$ and a linear decrease of vertical velocity, w, from its value at 1500 m to zero at the ocean bottom.

local plus planetary vorticity change, $\zeta_{end} - \zeta_{start} + \int_{start}^{end} dt\ v$, is compared with the time-integrated vortex stretching, $f\int_{start}^{end} dt\ \frac{\partial w}{\partial z}$. The errors in the vortex stretching are at least as large as the estimates while the errors in $\Delta\zeta + \beta\int v dt$ are $\pm.32 \times 10^{-6}$ due to measurement errors and $+.05 \times 10^{-6}$ due to sampling errors.

From MODE-1 measurements (Figure 1.2) at 420 m nominal depth vorticity is estimated for forty-eight sub-arrays consisting of three or four current meters (Figure 5.2). Errors in these estimates are $\pm.05 \times 10^{-6}$ sec^{-1} due to measurement errors and 16% due to sampling errors for an estimated average horizontal separation of 120 km. Divergence ratios, defined in Chapter III and calculated for these sub-arrays, varied from .2 to .5 with an average of .35, however, so that the estimates of vorticity may be in error by ±35%. Estimates of horizontal advection of relative vorticity are possible from these measurements. If the estimates of vorticity are in error by ±35%, however, estimates of horizontal advection have errors of $\pm 2.0 \times 10^{-12}$ sec^{-2} which are as large as the observed magnitude of local time changes of vorticity, 2×10^{-12} sec^{-2}.

Figure 5.2. Map of relative vorticity from MODE-1 measurements of velocity at 420 m depth during the period 21-28 April, 1973. Measurements on moorings 1, 2, 3, 5, 6, 7, 8, 9, 10, and 13 are used.

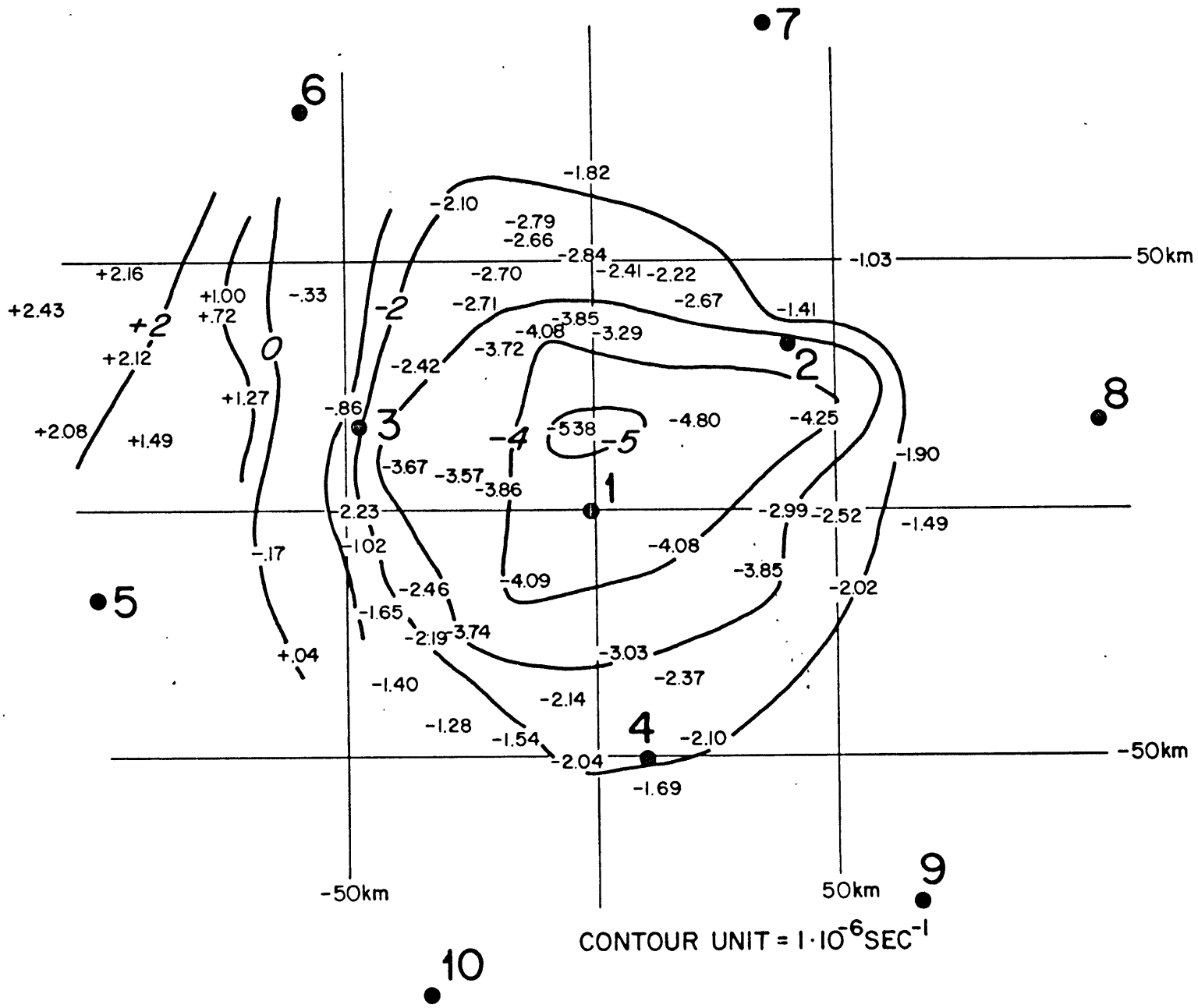
7
6
-1.82
-2.10
-2.79
-2.66
-2.84
-1.03
50km
+2.16
-2.70
-2.41
-2.22
+1.00
+.72
-.33
-2
-2.71
-2.67
-1.41
+2.43
+2
+2.12
0
-3.85
-4.08
-3.29
-3.72
-2.42
2
+1.27
-.86
3
8
+2.08
+1.49
-4
-5.38
-5
-4.80
-4.25
-1.90
-3.67
-3.57
-3.86
1
-2.23
-2.99
-2.52
-1.49
-1.02
-.17
-4.08
-3.85
-4.09
-2.46
-2.02
5
-1.65
-2.19
-3.74
-3.03
+.04
-2.37
-1.40
-2.14
-1.28
-1.54
4
-2.10
-2.04
-50km
-1.69
-50km
50km
9
10
CONTOUR UNIT = 1·10⁻⁶SEC⁻¹

RESULTS AND DISCUSSION

The correlation between estimates of local change of vorticity and of advection of planetary vorticity (Table 5.1) is -0.20 which is not significantly nonzero at an 80% confidence level. The correlation between estimates of local change plus planetary advection and of vortex stretching (Table 5.2) is 0.60 which is significantly nonzero at an 80% confidence level, but is not significant at a 95% level.

The change of vorticity over the measurement period, $-2.59 \times 10^{-6}{}^{+.31 \times 10^{-6}}_{-.38 \times 10^{-6}}$ sec^{-1} is significantly different from the vorticity change due to the time-integrated planetary advection, $-1.28 \times 10^{-6}{}^{+ .06 \times 10^{-6}}_{-..18 \times 10^{-6}}$ sec^{-1}. Thus there is significant imbalance between local time change of vorticity and advection of planetary vorticity. The planetary advection accounts for only half of the observed local change of vorticity. Though the observed vertical structure of horizontal currents resembles a first baroclinic mode (Gould, Schmitz and Wunsch; 1974), the hypothesis that these observations at 1500 m depth could be explained by barotropic Rossby waves is not unreasonable since the zero of horizontal velocity for the first baroclinic mode is at nearly 1500 m (Richman, 1972). Statistically, however, there is not a balance between local changes and planetary advection so these observations cannot be explained as manifestations of linear barotropic Rossby waves which require this balance (Longuet-Higgins, 1965).

The sum of local change plus planetary advection over the measurement period, $-1.11 \begin{smallmatrix}+.37\\-.32\end{smallmatrix} \times 10^{-6}$ sec^{-1}, is of opposite sign from the change in vorticity due to vortex stretching, $+1.00 \times 10^{-6}$ sec^{-1}. Because of the neglect of nonlinear terms in the heat balance (shown to be important for IWEX observations in Chapter IV), this estimate of vortex stretching has an error at least as large as its value. For this reason a test of balance between vortex stretching and the sum of local change plus planetary advection cannot be made. That the estimates are of opposite signs suggests that such a balance does not occur. Because of the method by which vortex stretching is estimated, the marginally significant correlation between estimates of vortex stretching and of the sum of local changes plus planetary advection is likely due to the expected correlation between warm water and negative vorticity above a level of no motion and not due to a balance of these terms in the vorticity equation.

Because there are measurements of velocity on only four moorings estimates of horizontal advection of relative vorticity are not possible from MODE-0 Array 1 measurements. Estimates of horizontal advection of relative vorticity are possible from MODE-1 measurements. From calculations of the divergence ratio, however, the estimates of vorticity have estimated errors of 35% and these errors produce errors in estimates of horizontal advection of relative vorticity as large as the observed changes of vorticity. The larger

errors in vorticity for MODE-1 measurements are attributed to larger errors in velocity caused by the variations in depth of current meters nominally at the same depth (Wunsch, Hogg and Richman, 1974). Because of instrument malfunctions estimates of vortex stretching are impossible. Thus, no vorticity balance calculations are made from MODE-1 measurements.

The imbalance between local changes of vorticity and planetary advection for the MODE-0 Array 1 observations is in conflict with the barotropic Rossby wave fit used by McWilliams and Flierl (1975) to explain these same observations. This conflict between the results of a direct balance test and of a linear wave fit demonstrates the danger in extending the wave analysis from a description of the spatial and temporal scales of the observed currents to a description of their dynamics. While the barotropic Rossby wave fit accounts for 78% of the amplitude of the observed current (McWilliams and Flierl, 1975), the vorticity dynamics implied by the waves are in error by a factor of two since planetary advection accounts for only half the observed time change of vorticity in the balance test.

Although the terms balancing the remainder of the local vorticity change could not be determined from these measurements, it is reasonable on the basis of the results of the heat balance in Chapter IV to expect that the nonlinear horizontal advection is important in the vorticity balance.

For nonlinear dynamics energy transfer may occur. In terms of the baroclinic instability model, the vorticity squared, called enstrophy, must also increase during growth of the perturbation wave. Multiplying the vorticity equation (5.1) by vorticity yields:

$$\frac{\partial}{\partial t}(\zeta^2/2) + (u\cdot\nabla\zeta)\zeta + \beta v\zeta = fw_z\zeta \qquad (5.3)$$

As enstrophy increases, $\frac{\partial}{\partial t}(\zeta^2/2) > 0$, the enstrophy production must be positive, $fw_z\zeta - \beta v\zeta - (u\cdot\nabla\zeta)\zeta > 0$. No accurate estimates of w_z or $u\cdot\nabla\zeta$ are available, but a correlation between time series of local change of vorticity and of planetary advection can be done. Minimum correlation, -.33, occurs when planetary advection leads local change by three days but this minimum is not significantly different from the correlation for zero time lag, -.20. The phase lag is consistent with growth of perturbation wave enstrophy by conversion of planetary enstrophy, the enstrophy contained in the rotating, spherical ocean. Because a significant, unknown term in the vorticity balance is not included, this enstrophy production calculation should be regarded cautiously. From a complete vorticity balance phase lags between local change of vorticity and planetary advection, horizontal advection of relative vorticity, and vortex stretching could be estimated so the net enstrophy production could be calculated.

It is possible to carry out an experiment from which estimates of each term in the vorticity balance (equation 5.1) can be estimated accurately. Such an experiment consists of five moorings, each instrumented with a current meter at 750 m depth, in the following array:

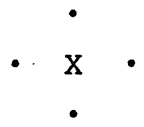

The horizontal spacing is 50 km and the central mooring (X) has two additional current meters also measuring temperature at 450 and 1050 m depths in order to estimate vortex stretching.

Estimates of vorticity from this array have errors of $\pm.09 \times 10^{-6}$ sec^{-1} due to measurement errors in velocity and may be small by 11% $(\frac{\partial v}{\partial x} - \frac{\partial u}{\partial y})$ due to sampling errors. These sampling errors are no larger than $.37 \times 10^{-6}$ sec^{-1} for values of $\frac{\partial v}{\partial x}, \frac{\partial u}{\partial y}$ of magnitude 1.7×10^{-6} sec^{-1}. Time derivatives of vorticity estimated from differences of five-day averaged vorticity then have errors no larger than $\pm 1.2 \times 10^{-12}$ sec^{-2}. Estimates of advection of planetary vorticity from this array have errors of $\pm.04 \times 10^{-12}$ sec^{-2} due to measurement errors and may be small by 19% due to sampling errors. As discussed in Chapter II, estimates of horizontal advection of momentum, $S^2 \frac{\partial \theta}{\partial x}$ or $S^2 \frac{\partial \theta}{\partial y}$ have errors of ±10% and ±.13 cm/sec/day due to measurement errors in speed and direction respectively and may be small by 11% due to sampling errors for $|\vec{k}| = 1/60$ km and separations

of 50 km. These errors become errors in horizontal advection of relative vorticity of $\pm.93 \times 10^{-12}$ sec^{-2}. Theoretical errors in estimates of horizontal advection are only $\pm.11 \times 10^{-12}$ sec^{-2}.

To estimate vortex stretching from these array measurements, it is assumed that the sum of local plus horizontally advective changes of temperature can be attributed to vertical advection of the mean vertical profile of temperature, as in equation 4.2, and not to the divergence of heat fluxes from higher-frequency motions. The error in these estimates of vertical velocity for five-day averaging intervals is ±.4 m/day due mostly to scatter in the T/S relationship discussed in Chapter IV. Estimates of vortex stretching obtained by differencing vertical velocities over a 300 m depth interval have errors of $\pm1.1 \times 10^{-12}$ sec^{-2}.

Thus, all terms in equation 5.1 can be estimated from this array with errors less than 1.2×10^{-12} sec^{-2}, which are smaller than 2×10^{-12} sec^{-1}, the expected magnitude for each of these terms based on scale analysis with U = 10 cm/sec, ω = 1/10 days, $|\vec{k}|$ = 1/60 km, N = 2.5 cph, and H = 1 km. This array consists of the minimum number of measurements needed to estimate the vorticity balance (equation 5.1). The number of moorings is one less than the six required to estimate all second derivatives. The use of horizontal non-divergence simplifies the estimation of horizontal advection of relative vorticity so that only five moorings are required.

From such array measurements the relative roles of horizontal advection, planetary advection and vortex stretching in causing local time changes of vorticity should be determined. Such an experiment would provide an understanding of the vorticity dynamics of eddy motions and guidance to theoretical modelers on the applicability of their models in explaining these motions. From these measurements energy transfer and enstrophy production also can be estimated. The phase lag between time series of local change and of horizontal advection of temperature on the central mooring determines the energy conversion as in Chapter IV. Phase lags between time series of local change of vorticity and of horizontal advection of relative vorticity, planetary advection and vortex stretching determine the enstrophy production.

CONCLUSIONS

Estimates of local time change of vorticity and of advection of planetary vorticity from MODE-0 Array 1 measurements are significantly not in balance. These observations then cannot be explained by barotropic Rossby waves which require a balance between local changes and planetary advection. A phase lag such that planetary advection leads local change of vorticity is consistent with growth of perturbation wave enstrophy by conversion of planetary enstrophy. Accurate estimates of horizontal advection of relative vorticity and of vortex stretching for vorticity balance cal-

culations are not possible from existing data so net enstrophy production cannot be estimated. An experiment is suggested from which estimates of local change of vorticity, horizontal advection of relative vorticity, advection of planetary vorticity, and vortex stretching can be made with errors small compared with the expected magnitudes of these terms so that vorticity balance calculations can be carried out. From this experiment both energy conversion and enstrophy production also can be estimated.

CHAPTER VI

CONCLUSIONS

This thesis presents tests for lowest-order balances in the conservation equations for horizontal momentum, mass, heat and vorticity. The chapter on each of these balance tests includes a conclusions section where the results are summarized. This last chapter outlines the results of all the balance tests and indicates their importance in understanding the dynamics of low-frequency currents.

Geostrophy is the lowest-order horizontal momentum balance within estimated errors for the MODE-1 measurements (Chapter II). Eighty-two percent of the thermal wind correlations between time series of horizontal temperature gradient and of vertical shear of horizontal current are significantly nonzero at a 99% confidence level with most of the nonsignificant correlations occurring at larger horizontal separations where the sampling errors are larger. Daily estimates of geostrophic current differences account for 92% of the variance in observed current differences. Thirty-two comparisons between observed and geostrophic current differences averaged over four days show geostrophic agreement within estimated three standard deviation errors. Only two comparisons fail to agree within two standard deviation errors. The standard deviation of the discrepancy between these observed and geostrophic current differences is

1.9 cm/sec which is 26% of the standard deviation of the observed current differences.

Horizontal nondivergence is the lowest-order mass balance within estimated errors for the MODE-0 Array 1 measurements (Chapter III). The correlation between daily estimates of $\frac{\partial u}{\partial x}$ and $\frac{\partial v}{\partial y}$ is -.95, significantly nonzero at a 99% confidence level. All twelve comparisons between four-day averaged estimates of $\frac{\partial u}{\partial x}$ and $\frac{\partial v}{\partial y}$ show agreement with horizontal nondivergence within estimated three standard deviation errors. Only one comparison, which occurs during a time period when estimates of $\frac{\partial u}{\partial x}$ and $\frac{\partial v}{\partial y}$ are changing rapidly, does not agree within two standard deviation errors. The standard deviation of estimates of horizontal divergence, which is the discrepancy from horizontal nondivergence, is $.22 \times 10^{-6}$ sec^{-1} which is 36% as large as the standard deviation of the horizontal derivatives of velocity.

These tests for geostrophy and horizontal nondivergence provide an observational basis for the lowest-order horizontal momentum and mass balances which has been lacking for low-frequency currents. These tests, however, contribute little to the understanding of current dynamics since geostrophy and horizontal nondivergence are expected on theoretical grounds. An extended error analysis shows that higher-order momentum balances and direct estimates of horizontal divergence should not be attempted until measurement errors are reduced significantly. These tests for geos-

trophy and horizontal nondivergence do indicate the validity of the measurement error estimates so that within these errors higher-order balances of heat and vorticity can be tested.

Tests of heat and vorticity balances are more valuable contributions to the understanding of the dynamics of low-frequency currents because the lowest-order balances are not theoretically well-established.

For the IWEX measurements the lowest-order heat balance is between local time changes of temperature and horizontal advection of temperature within estimated errors (Chapter IV). Estimates of horizontal advection account for 73% of the variance in local changes of temperature. This balance could be established only because a representation of horizontal advection of temperature in terms of the speed and turning about the vertical of horizontal current has small errors. The result of this balance test indicates that local changes of temperature are caused by advection of horizontally varying temperature features and not by vertical advection of the vertically-varying temperature field, as suggested by linear theory. The importance of horizontal advection is contrary to many interpretations of observations in this region as strictly linear waves. In terms of quasi-linear theory the magnitude of horizontal advection of temperature could be explained by linearizing about the forty-day averaged flow field. It could not be explained by advection by the long-time averaged mean flow

field, which is much smaller than the forty-day averaged flow field.

In the vorticity equation, MODE-0 Array 1 measurements are used to test for balance between local change of vorticity and advection of planetary vorticity, as would occur for barotropic Rossby waves (Chapter V). Planetary advection and local change of vorticity over the measurement period do not balance within estimated errors. Planetary advection balances approximately half of the local vorticity change, but there is a significant imbalance. This result directly contradicts the interpretation of these observations as manifestations of barotropic Rossby waves. An extended error analysis of the vorticity equation demonstrates that all terms in the vorticity balance (equation 5.1) can be estimated with errors smaller than the expected magnitudes of the terms from measurements on five moorings. These vorticity balance calculations would be useful in determining the importance of vortex stretching, planetary advection and horizontal advection in causing local changes of vorticity and could be used to arbitrate the applicability of two models with different vorticity balances in explaining observations.

Because the dominant questions in the dynamics of low-frequency currents involve energy transfer, indications of energy transfer within the context of a baroclinic instability model are sought. For the IWEX observations the minimum correlation between estimates of horizontal advection of temperature and local temperature change occurs when horizon-

tal advection leads local change by one day. This phase lag is consistent with the growth of a perturbation wave by conversion of the potential energy contained in the forty-day averaged flow field. For MODE-0 Array 1 observations the minimum correlation between estimates of planetary advection and local change of vorticity occurs when planetary advection leads local change by three days. This phase lag is consistent with the growth of perturbation wave enstrophy by conversion of planetary enstrophy. Longer time series are needed to establish the statistical significance of these phase lags and measurements at various horizontal spacings are needed to determine the scales of the currents involved in the energy transfer.

In order to observe eddy growth or decay during future ocean experiments these results should be used and extended to estimate statistically significant energy and enstrophy transfer. Such calculations require that the difference between local temperature change and negative horizontal advection of temperature be established as due to vertical advection and not to the divergence of heat fluxes from higher-frequency motions. They also require a complete local vorticity balance so the net enstrophy transfer can be estimated. Long time series of observations over a variety of horizontal separations are needed to isolate the temporal and spatial scales of the currents which act as source and sink for the eddy energy and enstrophy.

REFERENCES

Batchelor, G. K. (1960) The Theory of Homogeneous Turbulence, Cambridge University Press, London, 197 p.

Batchelor, G. K. (1967) An Introduction to Fluid Dynamics, Cambridge University Press, London, 615 p.

Briscoe, M. G. (1975) "Preliminary results from the tri-moored internal wave experiment (IWEX)", Journal of Geophysical Research, in press.

Bryan, K. (1974) "Can baroclinically unstable eddies be detected by hydrographic sections?", MODE Hot Line News, Woods Hole Oceanographic Institution unpublished document, 56, 1.

Bryden, H. L. (1974) "Geostrophic comparisons using moored current meter and temperature measurements", Nature, 251, 409-410.

Charney, J. G. (1973) "Planetary fluid dynamics", in Dynamic Meteorology (edited by P. Morel), Reidel Publishing Co., Boston, 97-351.

Eady, E. T. (1949) "Long waves and cyclone waves", Tellus, 1 (3), 33-52.

Fleagle, R. G. (1972) "BOMEX: an appraisal of results", Science, 176, 1079-1084.

Fofonoff, N. P. (1962) "Dynamics of ocean currents", in The Sea (edited by M. N. Hill), Interscience, New York, volume 1, 323-395.

Fofonoff, N. (1973) "Potential temperature/salinity curves from MODE-I CTD stations", MODE Hot Line News, Woods Hole Oceanographic Institution unpublished document, 43, 1.

Fofonoff, N. P., and H. Bryden (1975) "Specific gravity and density of seawater at atmospheric pressure", Journal of Marine Research, in press.

Freeland, H. (1975) "Divergence: objective analysis test", Dynamics and the Analysis of MODE-I: Report of the MODE-I Dynamics Group, Massachusetts Institute of Technology Department of Meteorology unpublished document, 28-30.

Freeland, H. J., P. B. Rhines, and T. Rossby (1975) "Statistical observations of the trajectories of neutrally buoyant floats in the North Atlantic", Journal of Marine Research, in press.

Gandin, L. S. (1965) Objective Analysis of Meteorological Fields, translated by Israel Program for Scientific Translations, Monson, Jerusalem, 242 p.

Gill, A. E., J. S. A. Green, and A. J. Simmons (1974) "Energy partition in the large-scale ocean circulation and the production of mid-ocean eddies", Deep-Sea Research, 21, 499-528.

Gould, W. J., and E. Sambuco (1975) "The effect of mooring type on measured values of ocean currents", Deep-Sea Research, 22, 55-62.

Gould, W. J., W. J. Schmitz, Jr., and C. Wunsch (1974) "Preliminary field results for a Mid-Ocean Dynamics Experiment (MODE-0)", Deep-Sea Research, 21, 911-931.

Green, J. S. A. (1960) "A problem in baroclinic stability", Quarterly Journal of the Royal Meteorological Society, 86, 237-251.

Green, J. S. A. (1970) "Transfer properties of the large-scale eddies and the general circulation of the atmosphere", Quarterly Journal of the Royal Meteorological Society, 96, 157-185.

Hayes, S. P. (1975) "The temperature and salinity fine structure of the Mediterranean Water in the Western Atlantic", Deep-Sea Research, 22, 1-11.

Hide, R. (1971) "On geostrophic motion of a non-homogeneous fluid", Journal of Fluid Mechanics, 49, 745-751.

Holland, W. R., and L. B. Lin (1975) "On the generation of mesoscale eddies and their contribution to the oceanic general circulation: I. A preliminary numerical experiment", Journal of Physical Oceanography, in press.

Horton, C., and W. Sturges (1975) "Comparison of velocity shear determined from STD observations and current meter observations at MODE mooring 3", (Abstract), EOS Transactions American Geophysical Union, 56, 377.

Iselin, C. O'D. (1936) "A study of the circulation of the Western North Atlantic", Papers in Physical Oceanography and Meteorology, 4 (4), 1-101.

Koshlyakov, M. N., and Y. M. Grachev (1973) "Meso-scale currents at a hydrophysical polygon in the tropical Atlantic", Deep-Sea Research, 20, 507-526.

Kung, E. C. (1973) "Note on design of an optimized computation scheme for kinematic vertical motion fields", Monthly Weather Review, 101, 685-690.

Kung, E. C. (1975) "Balance of kinetic energy in the tropical circulation over the Western Pacific", Quarterly Journal of the Royal Meteorological Society, 101, 293-312.

Longuet-Higgins, M. S. (1965) "Some dynamical aspects of ocean currents", Quarterly Journal of the Royal Meteorolcgical Society, 91, 425-451.

Malkus, W. V. R. (1964) "Boussinesq equations", Geophysical Fluid Dynamics Course Lectures and Seminars, Woods Hole Oceanographic Institution unpublished document, I, 1-12.

McWilliams, J. (1974) "MODE mean currents and eddy surface intensification", MODE Hot Line News, Woods Hole Oceanographic Institution unpublished document, 57, 1.

McWilliams, J. C., and G. R. Flierl (1975) "Optimal, quasi-geostrophic wave analyses of MODE array data", submitted to Deep-Sea Research.

McWilliams, J. C., and A. R. Robinson (1974) "A wave analysis of the Polygon array in the tropical Atlantic", Deep-Sea Research, 21, 359-368.

Millard, R., Jr., and H. Bryden (1973) "Spatially-averaged MODE-I CTD stations", MODE Hot Line News, Woods Hole Oceanographic Institution unpublished document, 43, 2.

Miller, E. H., and W. L. Thompson (1942) "A proposed method for the computation of the 10,000 foot tendency field", The University of Chicago Institute of Meteorology Miscellaneous Reports, 1, 10 p.

MODE Scientific Council (1973) "MODE-I: The program and the plan", Massachusetts Institute of Technology Department of Meteorology unpublished document, 38 p.

Müller, P. (1975) "A summary of theoretical studies on the interaction between short internal gravity waves and larger scale motions in the ocean", Dynamics and the Analysis of MODE-I: Report of the MODE-I Dynamics Group, Massachusetts Institute of Technology Department of Meteorology unpublished document, 139-148.

Panofsky, H. A. (1951) "Large-scale vertical velocity and divergence", in Compendium of Meteorology, edited by T. F. Malone, Waverly Press, Baltimore, 639-646.

Phillips, N. (1966) "Large-scale eddy motion in the Western Atlantic", Journal of Geophysical Research, 71, 3883-3891.

Pearson, E. S., and H. O. Hartley (editors) (1970) Biometrika Tables for Statisticians, volume 1, Cambridge University Press, London, 270 p.

Rasmusson, E. M. (1971) "BOMEX atmospheric mass and energy budgets: Preliminary results", BOMEX Bulletin, National Oceanic and Atmospheric Administration unpublished document, 10, 44-50.

Rhines, P. (1970) "Edge-, bottom-, and Rossby waves in a rotating, stratified fluid", Geophysical Fluid Dynamics, 1, 273-302.

Rhines, P. B. (1975) "Waves and turbulence on a beta-plane", Journal of Fluid Mechanics, in press.

Richman, J. (1972) "Vertical modal structure of currents", MODE Hot Line News, Woods Hole Oceanographic Institution unpublished document, 12, 1.

Riser, S. (1975) "Temperature events at MODE-I site moorings 1 and 8", MODE Hot Line News, Woods Hole Oceanographic Institution unpublished document, 71, 1.

Robinson, A. R., and J. C. McWilliams (1974) "The baroclinic instability of the open ocean", Journal of Physical Oceanography, 4, 281-294.

Schmitz, W. J., Jr. (1974) "Observations of low-frequency current fluctuations on the Continental Slope and Rise near Site D", Journal of Marine Research, 32, 233-251.

Shonting, D. H. (1969) "Rhode Island Sound square kilometer study 1967: flow patterns and kinetic energy distribution", Journal of Geophysical Research, 74, 3386-3395.

Sverdrup, H. U., M. W. Johnson, and R. H. Fleming (1942) The Oceans, Prentice-Hall, Englewood Cliffs, New Jersey, 1087 p.

Swallow, J. C. (1971) "The Aries current measurements in the western North Atlantic", Philosophical Transactions of the Royal Society of London, A, 270, 451-460.

Swallow, J. (1975) "Geostrophy: finite difference test from Minimode floats", Dynamics and the Analysis of MODE-I: Report of the MODE-I Dynamics Group, Massachusetts Institute of Technology Department of Meteorology unpublished document, 36-39.

Tarbell, S. A. (1975a) "A compilation of moored current meter observations (MODE-1 Array, 1973)", Woods Hole Oceanographic Institution unpublished data.

Tarbell, S. A. (1975b) "A compilation of moored current meter observations (IWEX Array, 1973)", Woods Hole Oceanographic Institution unpublished data.

Tarbell, S. A. (1975c) "A compilation of moored current meter observations (MODE-0 Arrays)", Woods Hole Oceanographic Institution unpublished data.

Veronis, G. (1973) "Large scale ocean circulation", Advances in Applied Mechanics, 13, 1-92.

von Arx, W. S. (1962) Introduction to Physical Oceanography, Addison-Wesley, Reading, Massachusetts, 422 p.

Whitham, G. B. (1963) "The Navier-Stokes equations of motion", in Laminar Boundary Layers, edited by L. Rosenhead, Clarendon Press, Oxford, 114-134.

Wunsch, C., N. Hogg, and J. Richman (1974) "Results from temperature-pressure recorders during MODE-I", MODE Hot Line News, Woods Hole Oceanographic Institution unpublished document, 50, 1.

Wüst, G. (1924) "Florida- und Antillenstrom", Veröffentlichungen des Instituts für Meereskunde an der Universität Berlin, 12, 48 p.

BIOGRAPHY AND PUBLICATIONS

The author was born on July 9, 1946 in Providence, Rhode Island. On the 12th of April, 1969 he married Cindy. A son, Cyrus, was born on November 29, 1974.

In addition to his studies in the Woods Hole Oceanographic Institution-Massachusetts Institute of Technology Joint Program, the author has also attended Dartmouth College, University of Washington, George Washington University, The Johns Hopkins University, and the University of Rhode Island and has worked for the USN Oceanographic Office and the USN Underwater Sound Laboratory.

Bryden, H. (1973) "New polynomials for thermal expansion, adiabatic temperature gradient and potential temperature of sea water", Deep-Sea Research, 20, 401-408.

Stommel, H., H. Bryden and P. Mangelsdorf (1973) "Does the Mediterranean outflow come from great depth?", Pure and Applied Geophysics, 105, 879-889.

Bryden, H. (1974) "Geostrophic comparisons using moored current and temperature measurements", Nature, 251, 409-410.

Fofonoff, N. P. and H. Bryden (1975) "Specific gravity and density of sea water at atmospheric pressure", Journal of Marine Research, in press.